© 2014. Published by The Company of Biologists Ltd | Development (2014) 141, 4598-4609 doi:10.1242/dev.113563

RESEARCH ARTICLE

Two-pore channels function in calcium regulation in sea star oocytes and embryos

Isabela Ramos[1,2], Adrian Reich[1] and Gary M. Wessel[1,*]

ABSTRACT

Egg activation at fertilization is an excellent process for studying calcium regulation. Nicotinic acid adenine dinucleotide-phosphate (NAADP), a potent calcium messenger, is able to trigger calcium release, likely through two-pore channels (TPCs). Concomitantly, a family of ectocellular enzymes, the ADP-ribosyl cyclases (ARCs), has emerged as being able to change their enzymatic mode from one of nucleotide cyclization in formation of cADPR to a base-exchange reaction in the generation of NAADP. Using sea star oocytes we gain insights into the functions of endogenously expressed TPCs and ARCs in the context of the global calcium signals at fertilization. Three TPCs and one ARC were found in the sea star (*Patiria miniata*) that were localized in the cortex of the oocytes and eggs. PmTPCs were localized in specialized secretory organelles called cortical granules, and PmARCs accumulated in a different, unknown, set of vesicles, closely apposed to the cortical granules in the egg cortex. Using morpholino knockdown of PmTPCs and PmARC in the oocytes, we found that both calcium regulators are essential for early embryo development, and that knockdown of PmTPCs leads to aberrant construction of the fertilization envelope at fertilization and changes in cortical granule pH. The calcium signals at fertilization are not significantly altered when individual PmTPCs are silenced, but the timing and shape of the cortical flash and calcium wave are slightly changed when the expression of all three PmTPCs is perturbed concomitantly, suggesting a cooperative activity among TPC isoforms in eliciting calcium signals that may influence localized physiological activities.

KEY WORDS: Two-pore channel, ADP-ribosyl cyclase, NAADP, Calcium, Sea star, Oocyte

INTRODUCTION

Calcium ions are versatile intracellular messengers. Its concentration within the cytoplasm is spatially and temporally controlled by sequestration in membrane-bound calcium compartments containing ion channels, exchangers and pumps, which in total are able to elevate cytoplasmic calcium levels over 1000-fold in less than 1 s, and then promptly re-sequester the calcium to restore its low resting levels. Many extracellular stimuli can mediate changes in cytoplasmic calcium levels through production of second messengers such as inositol trisphosphate (IP_3), cADPR (cyclic ADP ribose) and NAADP (nicotinic acid adenine dinucleotide phosphate) (Carafoli et al., 2001; Whitaker, 2006). NAADP has been found to trigger calcium release from acidic vesicles, rather than from the endoplasmic reticulum (ER) (Churchill et al., 2002; Morgan et al., 2011; Patel et al., 2011; Guse, 2012), through a new class of calcium channels: the two-pore channels (TPCs) (Brailoiu et al., 2009; Calcraft et al., 2009; Zong et al., 2009). The effect of calcium release from a small vesicle instead of from a continuous tubular network means that this mechanism may yield small localized calcium fluxes. Integration of the two pathways (local×global) is also likely considering the increased activity of various calcium channels when exposed to calcium (calcium-induced calcium release). NAADP has been implicated in several physiological processes such as secretion of digestive enzymes and insulin by the pancreas (Macgregor et al., 2007; Arredouani et al., 2010), contractility of the heart (Macgregor et al., 2007), activation of T-cells (Berg et al., 2000; Davis et al., 2012; Davis and Galione, 2013) and the acrosomal reaction in sperm (Arndt et al., 2014; Sánchez-Tusie et al., 2014). However, the diversity of molecular mechanisms resulting from different isoforms of TPCs and its role in calcium signaling has remained obscure.

TPCs accumulate in acidic organelles such as lysosomes (Brailoiu et al., 2009; Calcraft et al., 2009) and plant vacuoles (Peiter et al., 2005). Their sequence predicts a topology of two repeats of a six transmembrane (TM) domain connected by a cytosolic loop, and a luminal re-entrant loop between transmembrane domains 5 and 6 for each of the domains (Hooper et al., 2011). TPCs exist as three isoforms (TPC1-TPC3), but TPC3 is absent from the genomes of many well-studied animals, including humans, mice and rats (Brailoiu et al., 2010b). Even though TPCs have been shown, by different groups and techniques, to be calcium-permeant channels triggered by NAADP, recent studies have also suggested that TPCs function as Na^+-permeant channels (with a 10:1 Na^+:Ca^{2+} permeability) regulated by the phosphoinositide phosphatidylinositol 3,5 bisphosphate [PI(3,5)P_2] (Wang et al., 2012). TPCs have been proposed also to interact with mTOR, and participate in the adaptation to starvation (Cang et al., 2013). In addition, TPCs have been implicated in autophagy (Lu et al., 2013a,b) and cellular differentiation (Parrington and Tunn, 2014).

Concomitant to the discovery of TPCs, a family of ectocellular enzymes named ADP-ribosyl cyclases (ARCs) was identified as being able to change their enzymatic mode from nucleotide cyclization to generate cADPR, to a base-exchange reaction to generate NAADP. ARC enzymes are quite remarkable in several features, including their ectocellular localization in the plasma membrane or facing the lumen of cytoplasmic vesicles, and their catalytic differences/versatility. Different ARCs are able to produce cADPR and ADPR through the cyclization of NAD or NAADP and cADPR-2-phosphate through a base-exchange reaction in the presence of nicotinic acid and NADP (Lee, 2001, 2012). The regulation mechanisms and potential physiological relevance underlying differential ARC functions are mostly unknown.

A great deal of the early work on NAADP signals was accomplished with the use of the sea urchin intact egg and egg-homogenates, which are remarkably stable and able to faithfully replicate the intact egg in the release/uptake of calcium when

[1]Department of Molecular Biology, Cellular Biology, and Biochemistry, Brown University, Providence, RI 02912, USA. [2]Instituto de Bioquímica Médica, Universidade Federal do Rio de Janeiro, Rio de Janeiro, RJ 21941, Brazil.

*Author for correspondence (rhet@brown.edu)

Received 3 June 2014; Accepted 23 September 2014

Development (2014) 141, 4598-4609 doi:10.1242/dev.113563

challenged with different messengers and inhibitors. Three TPCs and four ARCs have been previously found and characterized in sea urchin eggs (Churamani et al., 2007, 2008; Davis et al., 2008; Ramakrishnan et al., 2010; Ruas et al., 2010). Here, we make use of an alternative model to investigate the NAADP toolkit – TPCs and ARCs – in their endogenous environment in the context of the calcium signals at fertilization. Unlike sea urchins, sea stars retain their full-grown oocytes in the gonads arrested at prophase I of meiosis. One-methyl adenine (1MeA) is the molecular trigger for resumption of meiosis (Kishimoto, 2011). As these oocytes can be cultured *in vitro* prior to re-activating meiosis, we explored the potential to induce molecular perturbations in the oocytes by intracellular delivery of morpholinos prior to fertilization, and then to test functionality of TPCs and ARC at fertilization and in early development.

RESULTS

Identification of TPCs and ARC from sea star ovaries

One ARC (PmARC) and three TPC isoforms (PmTPC1, PmTPC2 and PmTPC3) were found in ovarian transcriptomes of the sea star *P. miniata*. PmTPCs share 37-43% similarity with their correspondents from sea urchin and human, whereas PmARC shares slightly higher similarity with the sea urchin β-ARC or spARC2 (43%) and human CD38 (supplementary material Fig. S1). As expected for a member of the ADP-ribosyl cyclase superfamily, PmARC has a predicted N-terminal signal peptide that targets the protein into the secretory pathway (cleavage position between amino acids 20 and 21) and a short (~16 amino acids) transmembrane domain close to the C terminus, which is anticipated to be an extracellular enzyme bound to the plasma membrane. Other predicted post-translational modifications include three potential N-glycosylation sites (positions 46, 70 and 179) and a positive score for a C-terminal GPI anchor (−1.71, with a *P*-value of 2.19^{-3}) (supplementary material Fig. S1). Interestingly, from the 19 echinoderm species in our transcriptome database (including representation of each major taxon: brittle stars, feather stars, sea cucumbers, pencil urchins, sea stars and sea urchins), only in the sea urchin transcriptomes is more than one ARC isoform detected in the ovaries. For all other species, the ovaries seem to express only one ARC isoform (data not shown). The topologies of PmTPCs were also predicted as expected for members of the voltage-gated ion channel superfamily – two domains, each containing six transmembrane regions, connected by a cytosolic loop. The N terminus and C terminus are predicted to be cytosolic, whereas the short loops between transmembrane domains 1 and 2, and 3 and 4, and the putative pore-forming re-entrant loop between transmembrane domains 5 and 6 (for each domain) are predicted to be luminal (supplementary material Fig. S2). Previous examination of the amino acid sequences of the putative pore regions of TPCs from several animals has revealed two residues that are conserved in both pores and across species (Brailoiu et al., 2009). Further analysis of the TPC putative pores from our database shows that the same residues (F263 and L273 in domain 1 of the human TPC1) are also conserved throughout the echinoderm phylum (supplementary material Fig. S3).

PmTPCs are localized in internal membranes of the cortical granules, whereas PmARC accumulates in nearby vesicles in the egg cortex

All PmTPC and PmARC mRNAs could be amplified from the early stages of oogenesis through early embryogenesis, as shown by their relative expression levels measured by qPCR (supplementary material Fig. S4). However, no specific subcellular localization for any of the messages was observed in the oocytes, eggs (i.e. vegetal×animal poles) or embryo tissues by whole-mount *in situ* hybridization (supplementary material Fig. S5).

Affinity-purified antibodies against each of the PmTPC isoforms and PmARC were raised and used for immunoblotting and immunolocalization experiments. The anti-PmTPCs polyclonal antibodies label fragments from 72 to 130 kDa in sea star ovaries, oocytes and embryos, coincident with their expected amino acid content based molecular weights of 101 kDa (PmTPC1), 95 kDa (PmTPC2) and 96 kDa (PmTPC3). Intriguingly, anti-PmARC antibodies label consistently an endogenous fragment over 200 kDa, significantly greater than its predicted 35 kDa molecular weight (Fig. 1B). Treatments of the samples with lower heating temperatures (50°C) and different reducing agents (DTT or 2-mercaptoethanol) did not change the molecular weight of the endogenous PmARC reactivity (supplementary material Fig. S6B). Treatment of the endogenous PmARC with PNGaseF greatly decreased its running profile (to ~70 kDa), but N- and O-glycosylation alone still did not appear to account for the discrepancy in molecular weight (supplementary material Fig. S6C). To determine the identity of the antibody-positive band, the fragment was immunoprecipitated and analyzed by mass spectrometry. This test resulted in the confirmation of the band as PmARC (supplementary material Fig. S6D and Table S2). We conclude that the aberrantly running PmARC must be modified in multiple ways, in addition to glycosylation. Importantly, a similar pattern of migration (a high molecular reaction around 150 kDa) was previously observed for one of the sea urchin ARCs [β-ARC (Davis et al., 2008)]. The atypical pattern of migration of the endogenous PmARC may be explained by the presence of highly stable protein interactions, which may be a result of the enzyme oligomerization or heterotypic aggregation with other components. The human ARC CD38, for example, has recently been characterized to form tetrameric associations that are related to its activity and raft associations in human cell lines (Hara-Yokoyama et al., 2012).

Immunofluorescence colocalization experiments show that PmARC and PmTPCs proteins are found in the cortex of the oocytes and eggs, as previously observed for TPCs and ARCs in the sea urchin eggs. PmTPC2 protein accumulates later in embryogenesis, being widely distributed in the tissues of mid-gastrulating embryos, but still can be detected in oocytes and eggs (Fig. 1C). Anti-PmTPC immunolocalization in the eggs was performed with or without peptide blocking to assess immunostaining specificity (supplementary material Fig. S7) and PmARC/PmTPCs colocalizations were also performed with or without Triton-X100 permeabilization (supplementary material Fig. S8). Without permeabilization, the signals for the three PmTPCs were mostly lost, whereas the signal for PmARC could still be detected, indicating an extracellular localization for at least some of the PmARC and largely an intracellular localization for the PmTPCs. Intensity line plots of the overlapping fluorescence signals also indicate that, although both proteins are accumulated in the cortex, their signals do not completely overlap (supplementary material Fig. S9).

The subcellular localization of PmTPCs and PmARC was assessed using immunogold electron microscopy labeling in immature oocytes (Fig. 2). Using standard fixation/embedding conditions, Fig. 2A shows the cortex of the sea stars oocytes. Cortical granules, yolk granules, vacuoles, mitochondria and the vitelline layer can be recognized. The same sample was then processed for immunogold electron microscopy, and, as shown under a low magnification in Fig. 2B, the cortical granules and many of the other organelles can be identified. Fig. 2C shows an inset from Fig. 2B where the accumulation of gold particles in the

Development (2014) 141, 4598-4609 doi:10.1242/dev.113563

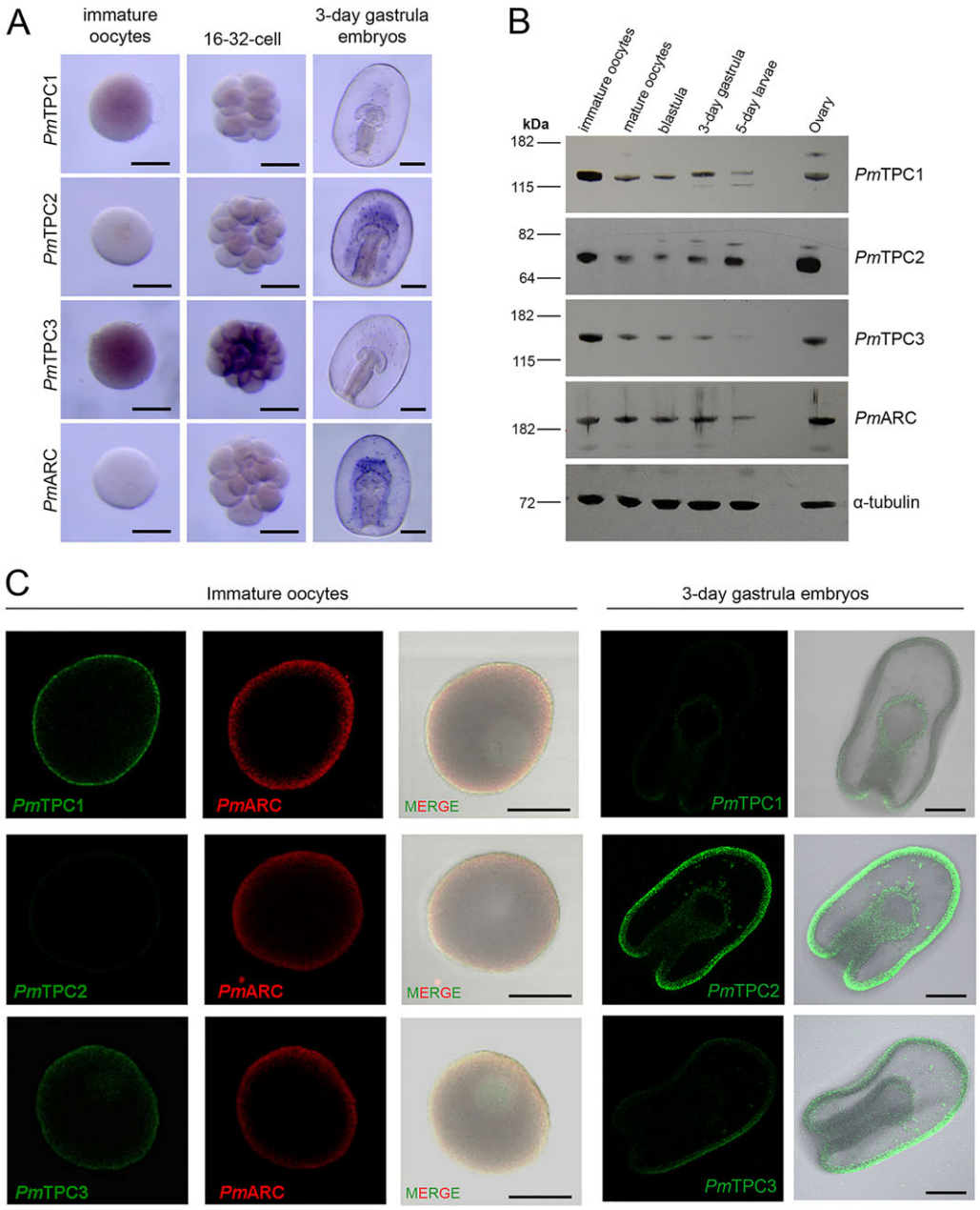

Fig. 1. PmTPCs and PmARC are enriched in the cortex of oocytes and eggs, and broadly distributed in embryos. (A) Whole-mount *in situ* hybridization for PmTPCs and PmARC in mature eggs and 16/32-cell embryos. (B) Immunoblotting for PmTPCs and PmARC in mature eggs, at different stages of development and in whole ovaries, as indicated. (C) Colocalization of PmTPCs and PmARC in the cortex of immature oocytes, and distribution of PmTPCs in 3-day gastrula embryos. Scale bars: 150 µm.

cortical granules after anti-PmTPC3 immunolocalization can be observed. PmTPC1 was also found in the cortical granules and in the plasma membrane (arrows) (Fig. 2D), and PmTPC3 was found mostly accumulated in the cortical granules (Fig. 2E). PmTPC3 and PmARC colocalization experiments show that PmARC is mainly found in another set of vesicles in the cortex of the oocytes, which are not the cortical granules, but are closely apposed to them (Fig. 2F,G, inset). Currently, we do not know the identity of this PmARC-positive vesicle, but ARC enrichment would be a useful metric to track its isolation. Some PmARC labeling in the plasma membrane was also detected. Gold particles for PmTPCs and PmARC labeling were quantified and are shown in Fig. 2H. Lack of antibodies suitable for immunogold labeling prevented analysis of endogenous PmTPC2 subcellular localization. Some labeling was found in the cortical granules, but insufficient densities to provide a proper quantitative analysis. The subcellular localizations of PmTPCs and PmARC do not change after oocyte maturation (data not shown).

Knockdown of PmTPCs and PmARC in the oocytes leads to abnormalities at fertilization and embryo lethality

Functional roles of PmTPCs and PmARC at fertilization and early embryogenesis were tested by suppressing their translation with specific morpholino antisense oligonucleotides. Immature oocytes were microinjected with specific morpholinos for each of the individual PmTPC isoforms or PmARC. Oocytes were injected, incubated for 36-48 h (to allow for turnover of the endogenous proteins) and then matured and fertilized *in vitro* (Fig. 3A).

Development (2014) 141, 4598-4609 doi:10.1242/dev.113563

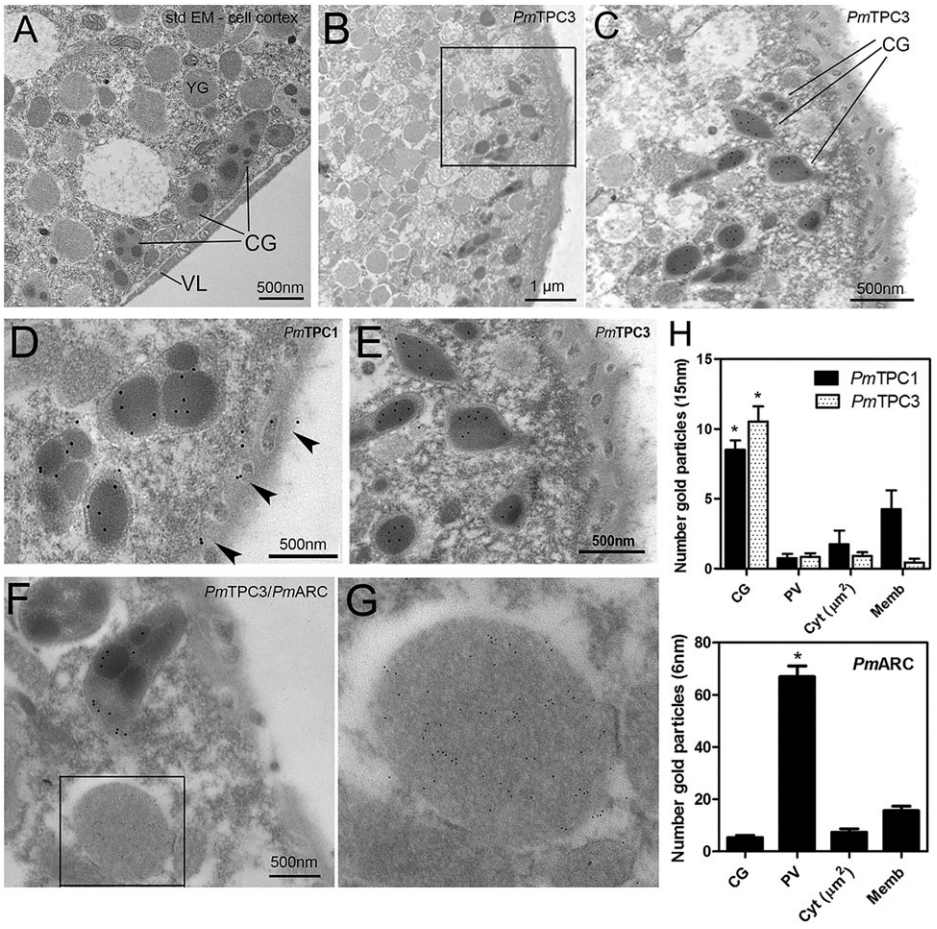

Fig. 2. PmTPCs and PmARC are enriched in different vesicles in the egg cortex.
(A) Standard TEM image of the immature oocyte cortex. VL, vitelline layer; CG, cortical granules; YG, yolk granule. (B) Low magnification image of the oocyte cortex processed for immunogold labeling with anti-PmTPC3 antibodies. Cortical granules are labeled. (C) Enlargement of boxed area in B. (D,E) Higher magnifications of the egg cortex showing the labeling of PmTPC1 (D) and PmTPC 3 (E) in the cortical granules and plasma membrane (arrowheads). (F) Colocalization of PmTPC3 (gold particle 10 nm) and PmARC (gold particle 6 nm) showing PmARC accumulation in another set of vesicles in the cortex of the oocyte. (G) Enlargement of boxed area in F. (H) Quantification of gold particles in the cortical granules (CG), peripheral vesicles (PV), cytoplasm (cyt) and plasma membrane. Graphs show the mean (±1 s.d.) of at least three experiments. *P<0.05, one-way ANOVA.

Knockdowns were assessed by immunoblotting before and after morpholino injections in the oocytes. In six out of 12 females, knockdowns were of 45±8% for PmTPC1, 64±12% for PmTPC2, 86 ±6% for PmTPC3 and 79±4% for PmARC (Fig. 3B). With the exception of PmTPC1, where morphants did not present any noticeable phenotypes, knockdown of PmTPC2, PmTPC3 and PmARC resulted in embryo lethality at the gastrula stage (~48 h after fertilization). Even though morphant embryos could go through cleavages and reach gastrulation (suggesting that polyspermy is not a cause of this phenotype), PmTPCs 2 and 3 knockdown eggs were not able to form and/or elevate the fertilization envelope properly, when compared with control-injected eggs after fertilization (Fig. 3C, arrowheads; see supplementary material Fig. S10 for quantifications).

The major contribution to the formation of the fertilization envelope comes from the cortical granules, where PmTPCs are localized. In echinoderms, these specialized secretory organelles are remarkably uniform in size, structure and content, as seen by the common internal substructure of electron-dense domains. In the purple sea urchin (*S. purpuratus*), the cortical granules contain material arranged in a spiral-lamellar structure, whereas in the starfish (*P. miniata*) these organelles enclose internal electron-dense circles (Fig. 2A; Holland, 1980; Oulhen et al., 2014). Upon fertilization, the cortical granules exocytose their contents in a calcium-dependent manner (the calcium wave at fertilization triggers the membrane fusion) and modify the vitelline layer to form the structure named the fertilization envelope. The fertilization envelope lifts off the plasma membrane, generating a physical block to polyspermy.

Ultrastructural analysis of the cortex of PmTPC3 knockdown eggs (2-5 min after fertilization) shows that cortical granule exocytosis is not affected, as the cortical granules cannot be seen in the peripheral cytoplasm anymore, and the fertilization envelope can be identified. This suggests that the contents of the cortical granules reacted with the components of the vitelline layer to form a modified framework (Fig. 3D). However, the structure of the fertilization envelope formed in PmTPC3 knockdown eggs is abnormal when compared with the fertilization envelope from control-injected eggs, with some domains not detached from the egg plasma membrane (Fig. 3D) and in some cases with the accumulation of cellular structures in the perivitelline space, probably as the result of abnormal exocytosis (supplementary material Fig. S11). To test the specificity of the PmTPC morpholino phenotype, additional morpholinos against PmTPC2 and PmTPC3 (directed to slightly different regions of the 5′UTR) and control morpholinos (irrelevant sequences to the TPCs) were also injected in the eggs, resulting in comparable knockdowns and phenotypes. In both cases, the eggs presented abnormalities in the formation and elevation of the fertilization envelope, but for PmTPC2 the eggs did not proceed to the first cleavage and for PmTPC3 the embryos presented a delay in development but gastrulating embryos seemed to be viable (supplementary material Fig. S12).

Knockdown of PmTPC isoforms individually and of PmARC do not result in changes in shape, timing and amplitude of the calcium dynamics at fertilization, whereas a combined PmTPC knockdown results in substantial abnormalities

As anticipated by the observation that the cortical granules fuse with the plasma membrane in PmTPC knockdown eggs, we also observed that the global calcium signals at fertilization are not altered when

Development (2014) 141, 4598-4609 doi:10.1242/dev.113563

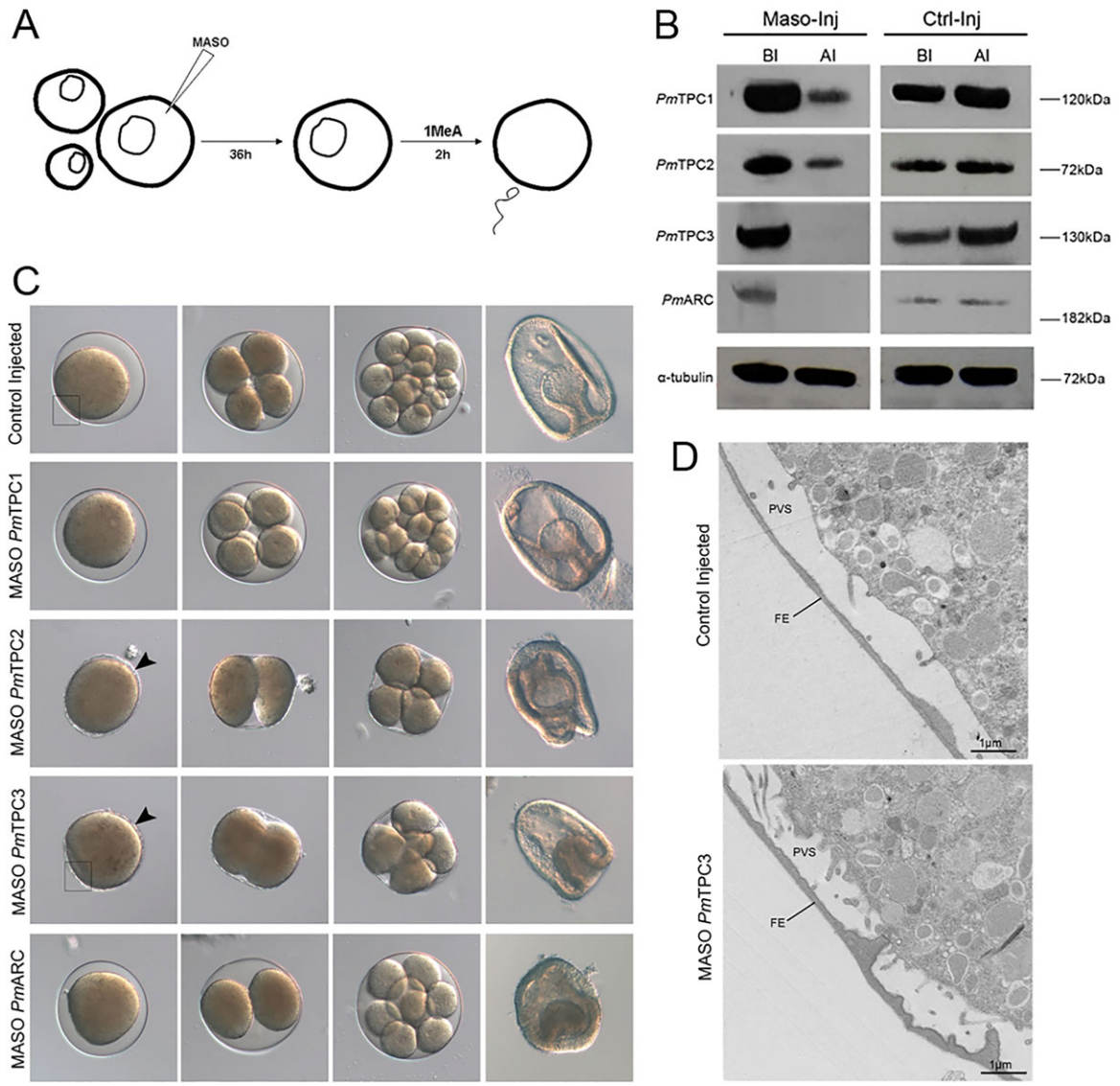

Fig. 3. PmTPCs and PmARC are essential for fertilization and early development. (A) Schematic representation of morpholino injections in immature oocytes followed by *in vitro* maturation and fertilization. (B) Immunoblotting of PmTPCs and PmARC knockdown before and after the morpholino injections. (C) Control and injected eggs, and embryos at first cleavage, 8-16 and 16-32 cell stages, and gastrulation. Arrowheads indicate the abnormal fertilization envelopes. (D) TEM images of control and PmTPC3 knockdown egg cortices showing the ultrastructural abnormalities in the formation and elevation of the fertilization envelope. FE, fertilization envelope; PVS, perivitelline space.

PmTPCs are knocked down individually in the oocytes. Fertilization in sea stars triggers a calcium cortical flash of ~5 s followed by a calcium wave that starts from the point of sperm interaction and takes about a minute to cross the entire egg. Total calcium re-uptake (fluorescence levels going back to background levels) takes about 10 min in control eggs (Fig. 4A, upper panel; Fig. 4B, black trace). Those signals are not significantly altered in terms of amplitude, timing and shape in PmTPC knockdown eggs after fertilization (Fig. 4A,B; supplementary material Movie 1). The same pattern was observed in PmARC knockdown eggs (data not shown).

To further investigate the participation of TPCs in the fertilization calcium signals, all three PmTPCs were knocked down concomitantly in the oocytes (Fig. 5B). The phenotypes in embryo lethality and in the fertilization envelope are reproduced (Fig. 5A), but the calcium signals at fertilization were altered in terms of shape and timing. In ~50% of the eggs co-injected with morpholinos directed against all three PmTPCs, the onset of the calcium wave after the cortical flash appeared twice, from two different points of origin, giving rise to two merging calcium waves starting only a few seconds apart from each other (Fig. 5C, upper panel; supplementary material Movie 1). Additionally, in one of the eggs tested, the cortical flash occurred after the onset of the calcium wave (Fig. 5C, lower panel; supplementary material Movie 1). However, the total amplitude of the abnormal calcium signals is comparable with the control single-wave signal (Fig. 5D), and are still able to trigger the fusion of the cortical granules, resulting in the formation of an abnormal fertilization envelope. Unfortunately, we were unable to test the effect of NAADP directly on the combined TPC knockdowns.

PmTPCs knockdown results in alkalinization of the cortical granules

Because the phenotype in the fertilization envelope is not resultant from abnormalities in the amplitude of the global calcium signals and/or abnormal cortical granules exocytosis, we hypothesized that

Development (2014) 141, 4598-4609 doi:10.1242/dev.113563

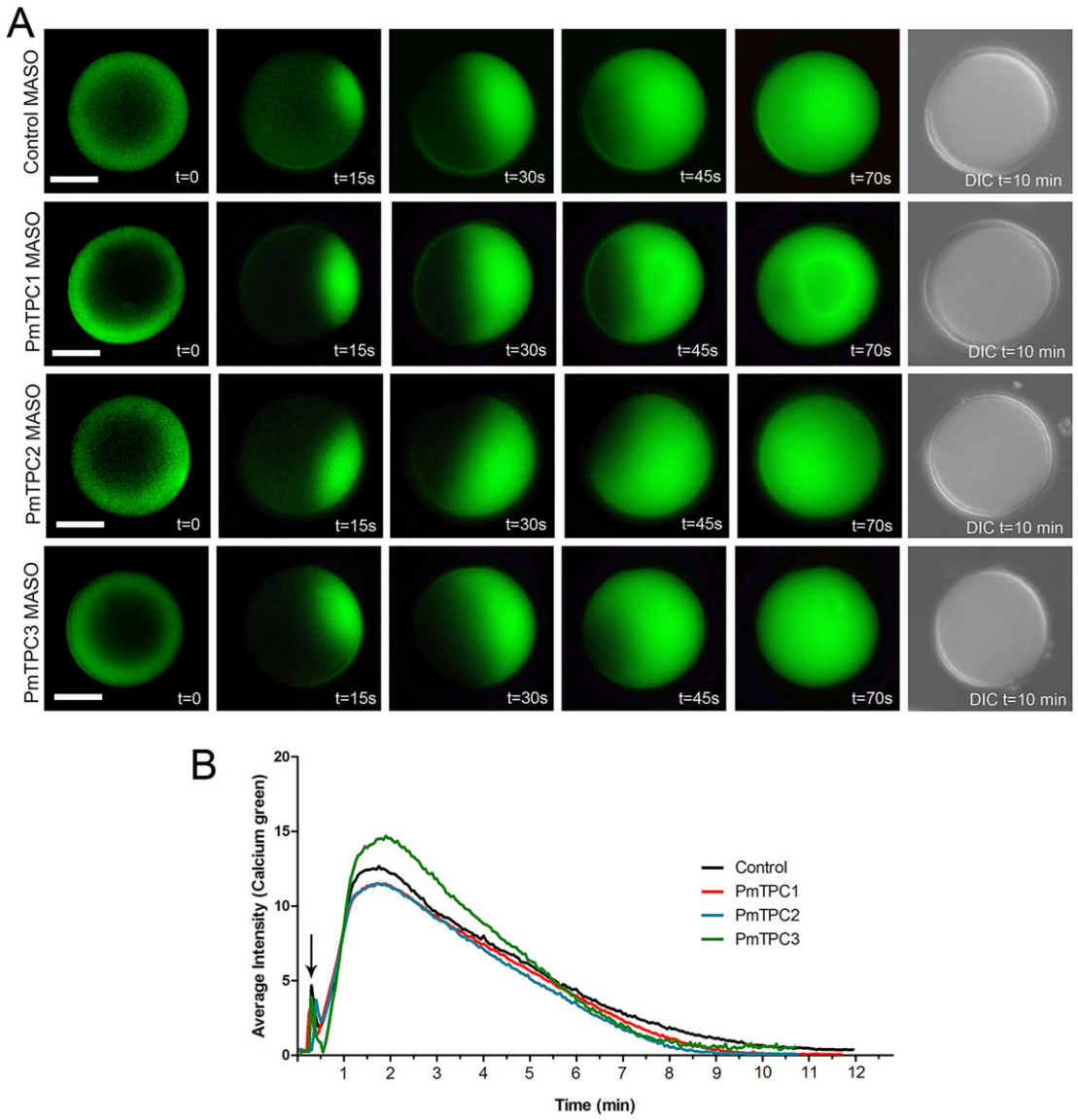

Fig. 4. TPCs have overlapping functions in the egg at fertilization: knockdown of PmTPCs individually does not alter major calcium fluxes at fertilization. (A) Immature oocytes were co-injected with Calcium green 10 kDa Dextran and each of the PmTPCs morpholinos. The cortical flash (*t*=0 s) and calcium wave at fertilization were monitored. (B) After the cortical flash (arrow), completion of the wave takes about 1 min and complete re-uptake of the released calcium takes about 10 min. Traces are representative of at least nine experiments. Scale bars: 100 µm.

knockdown of PmTPCs could be affecting the luminal pH of the organelles. NAADP-induced alkalinization of acidic organelles has been observed in sea urchin eggs (Morgan and Galione, 2007a,b; Morgan et al., 2013) and, more recently, changes in the pH of lysosomes were observed in cells overexpressing or silenced (shRNA) for TPC2 (Lu et al., 2013b). In this context, we learned that in sea star eggs, Lysosensor probes label specifically the cortical granules (Fig. 6A, upper panel and inset in the middle panel). The specificity was tested by fertilizing the labeled eggs, and, even though the fertilization envelope does not form properly (it is only partially lifted in some regions), it is possible to observe the loss in dye accumulation where the cortical granules fused to form the envelope (Fig. 6 lower panel, arrow). Thus, we used Lysosensor green DND-189 (pK_a~5.2) to measure changes in the cortical granules pH between control-injected and PmTPC knockdown eggs (Fig. 6B). As shown in Fig. 6C, PmTPC knockdown eggs seem to sustain an alkalinization of the cortical granules, when compared with control-injected eggs, an environment that may alter content function while in the granule.

DISCUSSION

Since the discovery of NAADP and the findings that it can mobilize calcium from the endolysosomal system, new insights into the functions of ARCs and TPCs in their endogenous environment have become crucial for the understanding of this localized signaling pathway. Electrophysiological studies in sea stars oocytes/eggs have demonstrated that NAADP participates in the response to sperm by triggering an initial calcium current. This leads to a change in membrane potential depolarizing the membrane to the threshold of activation for the voltage-gated calcium channels, which in turn allows a greater calcium influx that results in the cortical flash. It has also been shown that the injection of (caged) NAADP elicits a cortical calcium signal that is not affected by the downregulation of IP_3 receptors (Santella et al., 2000; Lim et al., 2001). Furthermore,

Development (2014) 141, 4598-4609 doi:10.1242/dev.113563

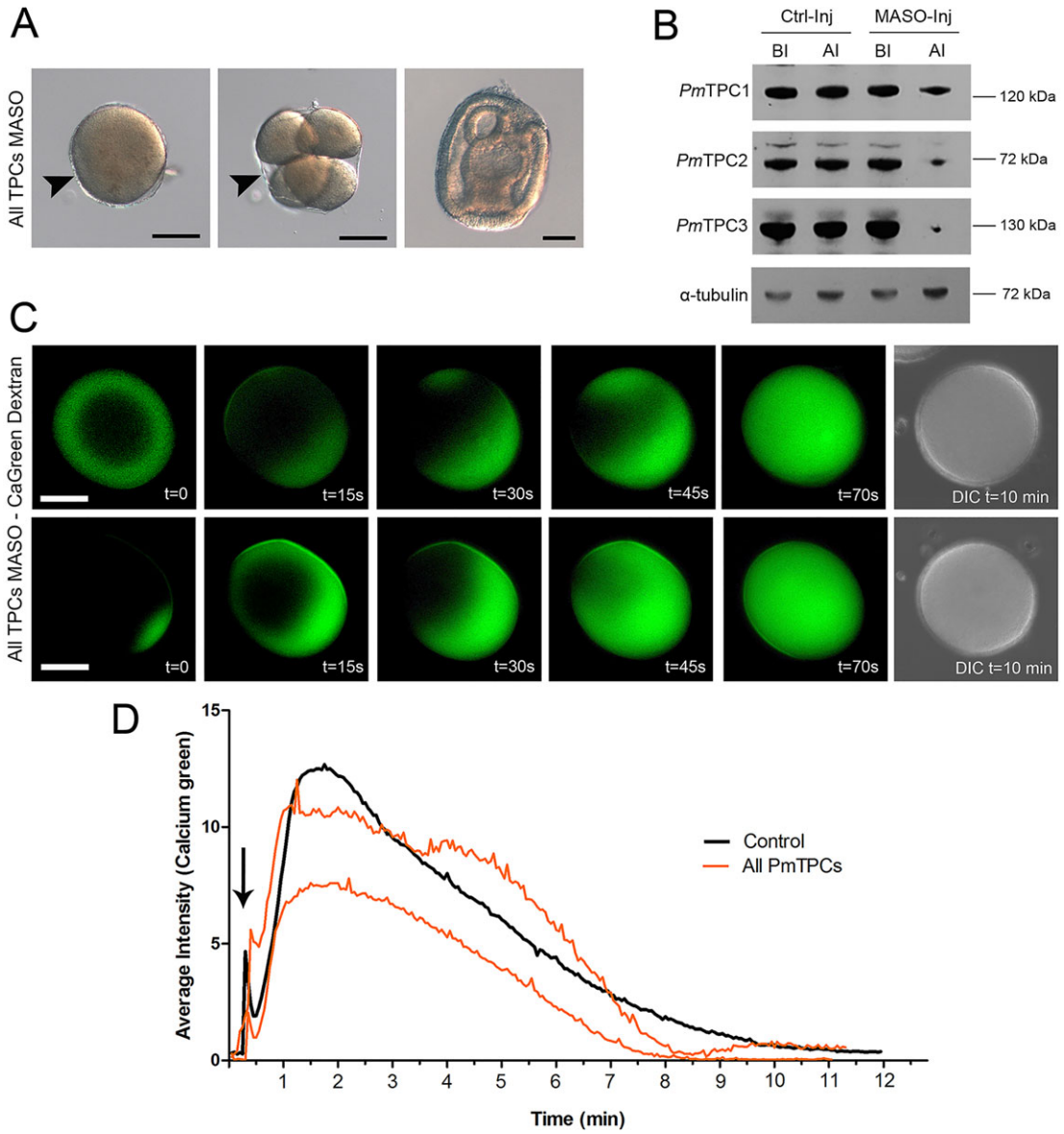

Fig. 5. TPCs have overlapping functions in the egg at fertilization: knockdown of all PmTPCs. (A) Embryos from oocytes co-injected with all three PmTPCs morpholinos. Arrowheads indicate the abnormal fertilization envelope. (B) Immunoblotting of PmTPCs knockdown before and after morpholino co-injections. (C) Calcium signals at fertilization were monitored after injection of Calcium green 10 kDa Dextran, and the two phenotypes for PmTPCs knockdown are shown. Scale bars: 100 µm. (D) Traces are representative of nine experiments, and refer to the knockdown eggs shown in C. Arrow indicates the cortical flash.

a link between NAADP-dependent membrane potential and the onset of the calcium wave was suggested. Evidence has accumulated that desensitization of NAADP receptors either prevents calcium release or impairs the pattern of sea star egg activation (Moccia et al., 2006a,b). Our findings that all three isoforms of PmTPCs and PmARC are found in the cortex of the oocytes/eggs support the contention that NAADP is involved in local cortical calcium signals at fertilization. Furthermore, in sea urchins, a peripheral ER is present in the cortex as a network that surrounds the cortical granules (Henson et al., 1990; Terasaki and Jaffe, 1991; Morgan et al., 2013). The cortical ER is contiguous with the ER in the bulk egg cytoplasm and forms closely apposed junctions with NAADP-targeted acidic organelles in the egg cortex, where bidirectional calcium signals have been shown to occur (Morgan et al., 2013). Thus, it seems reasonable to speculate that TPC-containing cortical granules in the sea star cortex may be one case where ER and acidic vesicle calcium signals amplify each other in a spatially organized manner.

However, the localization of PmTPCs and PmARC in different intracellular compartments (cortical granules×unidentified peripheral vesicles) is more difficult to resolve in terms of how these intracellular messengers and signals are regulated. In the sea urchin egg, two ARCs are associated with the cortical granules and a third one with the plasma membrane, facing the extracellular space (Davis et al., 2008). The sea urchin TPCs (SpTPC1, SpTPC2 and SpTPC3) are also in the cortex, but their subcellular localization is unknown (Ruas et al., 2010), as is the localization of the fourth sea urchin ARC (Churamani et al., 2008). Echinoderm cortical granules are membrane-bound organelles, members of the regulated family of secretory vesicles. TPCs have been localized to these types of organelles before, the paradigmatic example being the secretory granules of cytotoxic T lymphocytes, which have been shown to

Development (2014) 141, 4598-4609 doi:10.1242/dev.113563

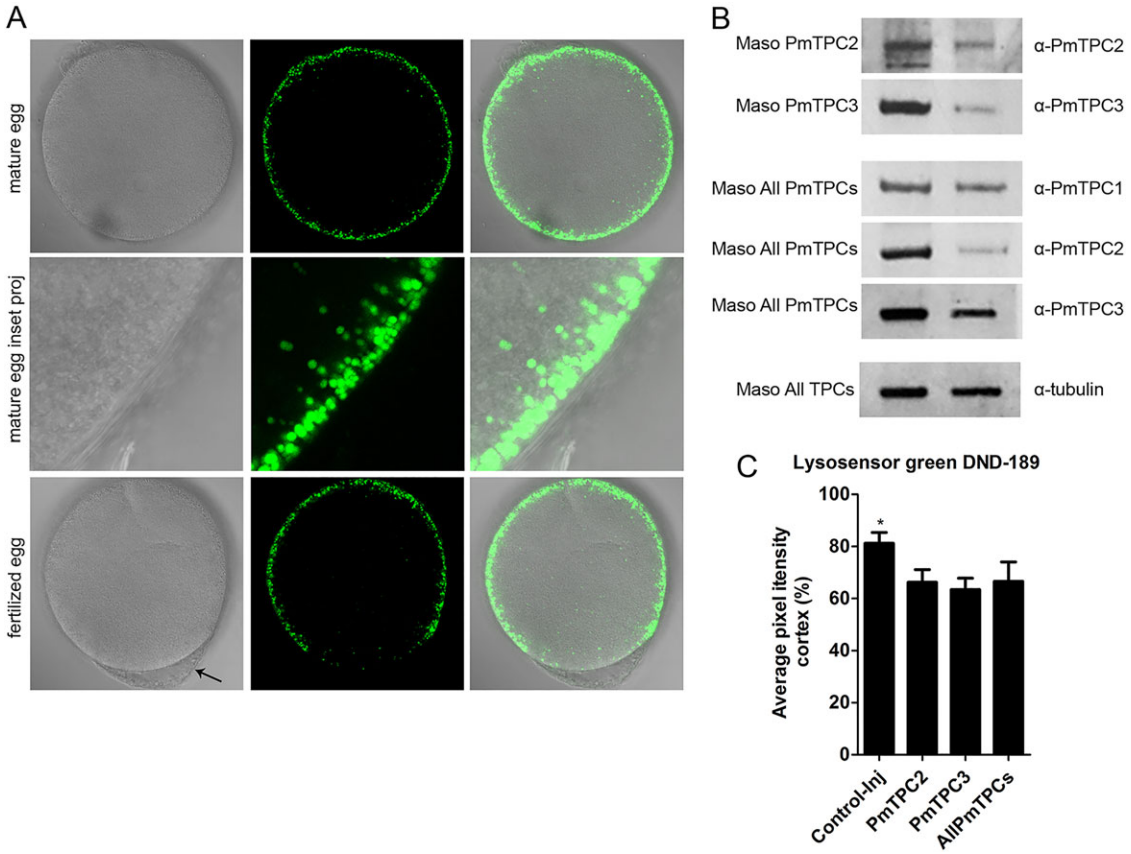

Fig. 6. PmTPC knockdown leads to increased pH in the cortical granules. (A) A mature egg labeled with lysosensor green DND-189 (upper panel). Projection of an inset in the egg cortex showing the cortical granules labeled with Lysosensor (middle panel). Labeled eggs were fertilized and the loss of Lysosensor accumulation in the regions where the cortical granules fused to form the envelope (arrow) illustrates the specificity of the Lysosensor labeling to the cortical granules (lower panels). (B) Immunoblotting showing the knockdown of PmTPCs after morpholino injections. (C) Lysosensor Green DND-189 fluorescence intensity of the egg cortex was measured using Metamorph. **P*<0.05, one-way ANOVA.

participate in the calcium release that triggers fusion of those organelles with the membrane during the immunological synapse (Davis et al., 2012; Davis and Galione, 2013). The presence of PmARC (an enzyme that synthesizes intracellular messengers) facing the lumen of a vesicle or the extracellular medium has been addressed before, and, at least in the sea urchin eggs and mammalian cells, it is likely that substrates and products can be transported inside and out of the ARC-positive organelle and from the outside of the plasma membrane to the cytoplasm (Guida et al., 2002; Churamani et al., 2007, 2008; Davis et al., 2008). The physiological relevance and evolutionary history of that arrangement is still not clear, and we cannot rule out the other possibility, of luminal production, transport and delivery of messengers by vesicle fusion – from an ARC-positive vesicle to a TPC-containing cortical granule, for example. It is noteworthy that intracellular vesicle movement is highly dynamic in the context of oogenesis. A growing oocyte is constantly endocytosing yolk molecules into yolk organelles and secreting components of the vitelline layer. Thus, vesicle movement, and fusion and crosstalk from vesicles of different intracellular routes are likely to be occurring continuously. Calcraft et al. (2009), for example, showed that the TPC-positive vesicles expressed in HEK cells are highly mobile.

The evidence that PmTPCs and PmARC are present in different compartments and that knockdown of PmTPCs impair proper formation of the fertilization envelope in the sea stars per se indicate that NAADP-dependent signals are likely to be completed in an intricate manner, where the production, transport and delivery of intracellular messengers is compartment regulated and the downstream signal generated may be a result of coupling of different targets. Additionally, the localization differences between sea urchin and sea stars TPCs and ARCs (number of expressed ARC isoforms and their localization) show that, regardless of how the signals are spatially regulated, they are not necessarily conserved in different species, given that even in the closely related sea urchins and sea stars, the localization and expression patterns of ARCs seem to differ substantially.

Even more intriguing than the spatial separation of PmTPCs and PmARC is the apparent localization of PmTPCs in internal membranes of the cortical granules. It appears that messengers would have to transpose an additional barrier to reach the TPCs in internal membranes, which could also be accomplished by transporters, and could represent an additional step of regulation of intracellular signals. In echinoderms, cortical granules are remarkably characteristic in terms of structure, content and organization, and can be easily identified by a typical internal substructure after standard TEM processing. In sea stars, as shown here and before (Holland, 1980; Reimer and Crawford, 1995), the cortical granules contain one or more electron-dense internal circles. Little is known about cortical granules biogenesis, or how the internal substructure is formed, but it has been extensively reported that the internal electron-dense regions accumulate different constituents (Hylander and Summers, 1982; Alliegro and Schuel, 1988; Wessel, 1989; Wessel et al., 2001). Predicted membrane proteins have been associated to those internal domains of cortical granules before; for example, RhoA, a member of

Development (2014) 141, 4598-4609 doi:10.1242/dev.113563

the Ras superfamily. Like PmTPCs, RhoA localizes to internal structures of the sea urchin cortical granules and is released in the perivitelline space after exocytosis (Cuéllar-Mata et al., 2000). The physiological relevance of those findings is still unknown. The presence of membrane-separated compartments within the cortical granules may represent a way to couple electrochemical gradients (much as it happens in mitochondria), assuming that other pumps, exchangers and channels are present in the membranes. Acidic stores, such as lysosomes, have been shown to sequester calcium by mechanisms that are dependent on their low luminal pH (Patel and Docampo, 2010), and have been increasingly implicated in elementary calcium signaling in several models (Patel and Muallem, 2011), including sea urchin eggs (Morgan, 2011). In egg homogenates, as in other cell types, the rationale for calcium storage/release into/out of acidic vesicles relates to the recurrent observations that inhibition of the vacuolar H^+-ATPase decreases proton uptake, and, if their membrane is sufficiently leaky, that alkalinization results in calcium release (Morgan and Galione, 2007a,b; Ramos et al., 2010). Thus, calcium uptake is thought to be driven by the proton gradient, probably coupled to a Ca^{2+}/H^+ exchanger. Although the detailed mechanisms are not well understood, it is known that different acidic vesicles are able to store/release calcium in sea urchin eggs (Morgan, 2011).

Another thought-provoking possibility to consider is the hypothetical involvement of the formation of lipid droplets enclosed by one single layer of phospholipids to facilitate the escape of polypeptides from the ER: the site of the synthesis of membrane proteins. Such a mechanism could explain the biogenesis of organelles enclosing membrane proteins into internal structures in a way that they are not defining internal compartments, but are shuttling membrane proteins inside the cell by carrying lipid droplets (Ploegh, 2007).

The assumption that ion movement in acidic vesicles may be coupled between pumps and exchangers lead us to the speculation that changes in pH (resulting from the PmTPCs knockdown) may be somehow linked with the problems in the formation of the fertilization envelope. Our decision to test the cortical granules pH was encouraged by: (1) our observations that individual PmTPC1, PmTPC2 and PmTPC3 knockdown does not result in significant changes in the ability of the eggs to elicit the global calcium signals at fertilization (it is true that knockdown of the three PmTPCs together leads to slight changes in the timing and shape of the calcium flash and wave, but the signals are still able to trigger the fusion of the cortical granules, and to form an abnormal fertilization envelope); (2) NAADP-induced alkalinization of acidic organelles have been observed in sea urchin eggs (Morgan and Galione, 2007a,b) and, more recently, changes in the pH of lysosomes were observed in cells overexpressing or silenced (shRNA) for TPC2 (Lu et al., 2013b). As a result, it emerges that the sea star cortical granules in TPC knockdown oocytes seem to sustain a slight pH alkalinization, which may be responsible for the problems in the formation and elevation of the fertilization envelope. The cortical granules have their contents specifically packed during oogenesis and exocytose in response to elevated calcium concentrations (much like secretory granules of somatic cells) (Wessel et al., 2001). The major function of the cortical granules exocytosis is to modify the existing oocyte/egg extracellular matrix (vitelline layer) to form the fertilization envelope. Several types of molecules responsible for the reaction that leads to the envelope formation are synthesized. These include enzymes such as ovoperoxidase, proteases, glycosidase and structural proteins like SFE9 and protealiasin (Wessel et al., 2001; Oulhen et al., 2013). Thus, changes in pH may result in problems in enzymatic reactions, giving rise to an abnormal structure in the fertilization envelope.

TPCs have been described as calcium channels activated by NAADP. Those properties have been observed by a collection of techniques such as pull-down of radioactive NAADP (Calcraft et al., 2009), electrophysiological analysis (Brailoiu et al., 2010a; Pitt et al., 2010; Schieder et al., 2010; Rybalchenko et al., 2012) mutations of the putative TPC pore region (Brailoiu et al., 2009, 2010a; Rybalchenko et al., 2012) and re-targeting of TPCs to the plasma membrane (Brailoiu et al., 2010a). However, recently, the possibility of TPCs functioning as Na^+-permeant channels (with a 10:1 Na^+:Ca^{2+} permeability) regulated by the phosphoinositide phosphatidylinositol 3,5 bisphosphate [$PI(3,5)P_2$] and not by NAADP (Wang et al., 2012) has been explored. The possibility of a high Na^+ selectivity in PmTPCs cannot be ruled out (Morgan and Galione, 2014), and may be the reason why we observed such small changes in the fertilization calcium signals after knockdown. Accordingly, the link between PmTPCs and NAADP and/or $PI(3,5)P_2$ remains unknown in sea stars oocytes and eggs.

MATERIALS AND METHODS

Animals and oocytes

Sea stars (*Patitria miniata*) were purchased from South Coast Bio Marine marine biological supply and maintained in circulating cold artificial seawater (16°C, Instant Ocean). Immature oocytes were handled as described previously (Wessel et al., 2010).

Identification of PmARC and PmTPC isoforms

Total RNA from *P. miniata* ovaries was extracted using Trizol reagent (Invitrogen) and first-strand cDNA synthesis was carried out using the M-MLV RT-PCR system with Platinum Taq High Fidelity (Invitrogen). Partial starting sequences for echinoderm ARCs and TPCs were retrieved from ovary *de novo* transcriptomes (A.R., unpublished) assembled using Agalma (version 0.3.5, https://bitbucket.org/caseywdunn/agalma) (Dunn et al., 2013). Full-length sequences of *P. miniata* ARC and TPCs were obtained after 3′ and 5′ RACE, using the BD SMART RACE cDNA amplification kit (BD Biosciences) with the primers listed in supplementary material Table S1.

Whole-mount RNA *in situ* hybridization

Sequences used to make antisense probes for PmARC, PmTPC1, PmTPC2 and PmTPC3 were amplified from ovary cDNA and cloned into pGEMT-EZ (Promega). The primers used for amplification are listed in supplementary material Table S1. The pGEMT-EZ plasmids were linearized using either *Nde*I (for T7 transcription) or *Apa*I (for SP6 transcription) (Promega). Antisense DIG-labeled RNA probes were constructed using a DIG RNA labeling kit (Roche). A non-specific DIG-labeled RNA probe complementary to neomycin from *Streptomyces fradiae* was used as a negative control. Samples were imaged on a Zeiss Axiovert 200M microscope equipped with a Zeiss color AxioCam MRc5 camera.

Production and purification of anti-PmTPC antibodies

Antibodies specific for the three PmTPC isoforms were raised commercially (with AbGent) by immunizing rabbits simultaneously with three specific hydrophilic peptides derived from predicted cytosolic regions of each of the PmTPCs. All peptides are listed in supplementary material Table S1. Specific antibodies were affinity purified from the immunized rabbit sera with the peptides cocktail (1 mg/ml each) conjugated to agarose beads using the Aminolink Plus immobilization kit from Thermo Scientific.

Recombinant PmARC bacterial expression, and production and purification of anti-PmARC antibodies

A 6×His fusion of a PmARC soluble fragment (lacking the signal peptide and the C terminal transmembrane domain) was expressed in *E. coli* strain BL21-Codon Plus (DE3) by induction with 1 mM IPTG for 6 h at 37°C. The bacterial

Development (2014) 141, 4598-4609 doi:10.1242/dev.113563

pellet was resuspended in 20 mM HEPES, 100 mM NaCl and 8 M urea (pH 8.0) supplied with a protease inhibitors cocktail (Roche). The lysate was clarified by centrifugation at 10,000 ***g*** for 20 min at 4°C and the recombinant PmARC was purified using a ProBond nickel column (Invitrogen).

Antibodies against rPmARC were raised commercially (with Cocalico Biologicals) by immunizing guinea pigs with 200-700 µg of rPmARC. Specific antibodies were affinity-purified from the immunized guinea pig sera using 500 µg rPmARC conjugated to agarose beads using the Aminolink Plus immobilization kit from Thermo Scientific.

Immunoblotting

Proteins were resolved in 4-10% gradient SDS-PAGE, blotted onto nitrocellulose membranes and immunolabeled as described previously (Oulhen et al., 2014). Primary affinity-purified antibodies were used at a 1:200 dilution. For morpholino knockdown blots, 26-32 oocytes were loaded per lane, depending on the experiment. α-Tubulin was also used as a loading control and detected using the monoclonal anti-α-tubulin clone B-5-1-2 (Sigma).

Immunolabeling TPCs and ARCs *in situ* by fluorescence

Oocytes and embryos were cultured as described above and samples were collected at indicated stages of development for whole-mount antibody labeling as described previously (Oulhen et al., 2014). For labeling, embryos were incubated overnight at 4°C with affinity-purified PmTPC1, PmTPC2, PmTPC3 and PmARC antibodies diluted (1:50) in blocking buffer. The samples were washed and then incubated with secondary anti-rabbit and anti-guinea pig Alexa 568 nm polyclonal antibodies (1:300) in PBST-BSA for 1 h at room temperature. Samples were mounted in Fluoromount G and imaged on a Zeiss LSM 510 laser scanning confocal microscope. For peptide block, 1 mg/ml of the three peptides for each of the PmTPCs were diluted in blocking buffer and added to the primary antibody incubations. For non-permeabilized samples, PBS and PBS-BSA (without Tween) were used for all incubations.

Microinjections of morpholino antisense oligonucleotides

Morpholino antisense oligonucleotides directed against the PmARC, PmTPC1, PmTPC2 and PmTPC3 5′UTRs were synthesized by Gene Tools and microinjected as described previously (Oulhen et al., 2014). Oocytes were incubated for 36-48 h after the injections and then matured *in vitro* and fertilized. Quantifications of the elevation of the fertilization envelopes and monitoring of the timing of development were carried out using a pool of 30-50 oocytes per experiment (n=6). Morpholino sequences are listed in supplementary material Table S1.

Standard and immunogold electron microscopy

For conventional transmission electron microscopy, all samples were fixed in freshly prepared 4% formaldehyde, 2.5% glutaraldehyde (Grade I) diluted in artificial sea water at 4°C for 24 h, and then embedded in epoxy resin, sectioned and stained using standard methods. For immunogold electron microscopy samples were fixed in 0.2-0.5% glutaraldehyde, 4% freshly prepared formaldehyde and embedded in LR-White resin at 4°C. Polymerization was carried out at room temperature under UV radiation for 96 h. Ultrathin sections were collected on nickel grids, incubated in 100 mM NH_4Cl in TBS for 30 min, and transferred to blocking buffer for 30 min at room temperature. Grids were incubated with the primary anti-PmTPCs and/or PmARC antibodies diluted 1:30 in the same buffer for 1 h. After washing, grids were incubated with 15 nm and/or 6 nm gold-labeled goat anti-rabbit and/or goat anti-guinea pig IgG (Electron Microscopy Sciences) diluted 1:60 for 1 h at room temperature. The sections were washed, stained in uranyl acetate and observed using a Philips 410 transmission electron microscope operating at 80 kV. Gold particles were quantified in five fields from at least three experiments.

Calcium imaging

For detection of the cortical flash and the fertilization calcium wave, the calcium fluorescent dye Calcium Green-1 coupled to a 10 kDa dextran (Molecular Probes) was injected into the cytoplasm of immature oocytes by pressure, using a Femto Jet injection system (Eppendorf), at a concentration of 5 mg/ml in the injection buffer [450 mM potassium chloride, 10 mM HEPES (pH 7.4)], as previously described (Moccia et al., 2006b). When used individually, PmTPC1, PmTPC2 and PmTPC3 morpholinos were added to the same solution at a concentration of 1.2 mM in the injection solution. When co-injected, final concentrations of the morpholinos were 0.4 mM in the injection solution. The injected oocytes were incubated for 36-48 h, matured *in vitro* and fertilized at the beginning of the recordings in the microscope. Cytosolic calcium changes were measured every 500 ms with a CCD camera (ORCA Hammamatsu) mounted on a Zeiss Axiovert 100 microscope with a Plan-Neofluar 20×/0.50 objective and a standard set of FITC filters. Fluorescence images were processed using Metamorph as previously described (Moccia et al., 2006b). Experiments were carried out using a pool of at least 30 oocytes per experiment.

PmARC immunoprecipitation and mass spectrometry

Ovaries were homogenized in PBS 1% Triton X-100 supplied with a protease inhibitors cocktail (Roche) and centrifuged 100,000 ***g*** for 1 h at 4°C. The supernatant was used as input for immunoprecipitation. Samples were pre-cleared with 100 µl of protein A conjugated with magnetic beads (Dynabeads, Invitrogen) for 30 min at 4°C. Cleared samples were incubated with anti-PmARC antibodies (1:200 dilution) for 1 h and the beads were added for an additional hour. Immunoprecipitated samples were resuspended directly in SDS-PAGE loading buffer for immunoblotting or silver staining for mass spectrometry. For mass spectrometry, the gel band corresponding to the molecular weight of the immunoprecipitated fragment was cut and proteins were digested using the In gel tryptic digestion kit (Pierce). Gel pieces were digested overnight at 37°C in the presence of 10 ng/µl trypsin. Samples were identified using a Thermo-Finnigan LTQ linear ion trap mass spectrometer using our *P. miniata* transcriptome database for peptides matching with MASCOT.

Deglycosylation

For deglycosylation analysis, immature oocytes were directly resuspended in lysis buffer and treated with PNGaseF (New England Biolabs) following manufacturer's instructions. Ovalbumin was used as positive control and reactions were incubated for 8 h at 37°C.

Lysosensor Green DND-189 and the cortical granules pH measurement

Immature oocytes were microinjected with different morpholinos and incubated for 36-48 h as previously described. Lysosensor green DND-189 (1 mM) was then diluted in the filtered sea water and oocytes were incubated for an additional hour at 16°C. The oocytes were then washed twice in filtered sea water and imaged on a Zeiss LSM 510 laser scanning confocal microscope using a default FITC filter set and a 488 nm Argon Laser. The average fluorescence intensities in the cortex of the oocytes were measured using Metamorph and plotted as relative values for each of the experiments.

Acknowledgements

We thank all members of the PRIMO lab for the rich work environment and the PEW foundation.

Competing interests

The authors declare no competing financial interests.

Author contributions

I.R. performed most of the experiments and participated in planning and writing of the paper. A.R. carried out the transcriptomes, assisted with cloning and sequencing, and with the design of the study. G.W. designed the study and participated in planning and writing of the paper.

Funding

I.R. was funded by the Program of Latin American PEW fellows. We are also grateful for support from the National Institutes of Health USA [2R01HD028152 to G.M.W.]. Deposited in PMC for release after 12 months.

Supplementary material

Supplementary material available online at
http://dev.biologists.org/lookup/suppl/doi:10.1242/dev.113563/-/DC1

Development (2014) 141, 4598-4609 doi:10.1242/dev.113563

References

Alliegro, M. C. and Schuel, H. (1988). Immunocytochemical localization of the 35-kDa sea urchin egg trypsin-like protease and its effects upon the egg surface. *Dev. Biol.* **125**, 168-180.

Arndt, L., Castonguay, J., Arlt, E., Meyer, D., Hassan, S., Borth, H., Zierler, S., Wennemuth, G., Breit, A., Biel, M. et al. (2014). NAADP and the two-pore channel protein 1 participate in the acrosome reaction in mammalian spermatozoa. *Mol. Biol. Cell* **25**, 948-964.

Arredouani, A., Evans, A. M., Ma, J., Parrington, J., Zhu, M. X. and Galione, A. (2010). An emerging role for NAADP-mediated Ca^{2+} signaling in the pancreatic β-cell. *Islets* **2**, 323-330.

Berg, I., Potter, B. V. L., Mayr, G. W. and Guse, A. H. (2000). Nicotinic acid adenine dinucleotide phosphate (NAADP(+)) is an essential regulator of T-lymphocyte Ca (2+)-signaling. *J. Cell Biol.* **150**, 581-588.

Brailoiu, E., Churamani, D., Cai, X., Schrlau, M. G., Brailoiu, G. C., Gao, X., Hooper, R., Boulware, M. J., Dun, N. J., Marchant, J. S. et al. (2009). Essential requirement for two-pore channel 1 in NAADP-mediated calcium signaling. *J. Cell Biol.* **186**, 201-209.

Brailoiu, E., Rahman, T., Churamani, D., Prole, D. L., Brailoiu, G. C., Hooper, R., Taylor, C. W. and Patel, S. (2010a). An NAADP-gated two-pore channel targeted to the plasma membrane uncouples triggering from amplifying Ca2+ signals. *J. Biol. Chem.* **285**, 38511-38516.

Brailoiu, E., Hooper, R., Cai, X., Brailoiu, G. C., Keebler, M. V., Dun, N. J., Marchant, J. S. and Patel, S. (2010b). An ancestral deuterostome family of two-pore channels mediates nicotinic acid adenine dinucleotide phosphate-dependent calcium release from acidic organelles. *J. Biol. Chem.* **285**, 2897-2901.

Calcraft, P. J., Ruas, M., Pan, Z., Cheng, X., Arredouani, A., Hao, X., Tang, J., Rietdorf, K., Teboul, L., Chuang, K.-T. et al. (2009). NAADP mobilizes calcium from acidic organelles through two-pore channels. *Nature* **459**, 596-600.

Cang, C., Zhou, Y., Navarro, B., Seo, Y.-j., Aranda, K., Shi, L., Battaglia-Hsu, S., Nissim, I., Clapham, D. E. and Ren, D. (2013). mTOR regulates lysosomal ATP-sensitive two-pore Na(+) channels to adapt to metabolic state. *Cell* **152**, 778-790.

Carafoli, E., Santella, L., Branca, D. and Brini, M. (2001). Generation, control, and processing of cellular calcium signals. *Crit. Rev. Biochem. Mol. Biol.* **36**, 107-260.

Churamani, D., Boulware, M. J., Geach, T. J., Martin, A. C. R., Moy, G. W., Su, Y.-H., Vacquier, V. D., Marchant, J. S., Dale, L. and Patel, S. (2007). Molecular characterization of a novel intracellular ADP-ribosyl cyclase. *PLoS ONE* **2**, e797.

Churamani, D., Boulware, M. J., Ramakrishnan, L., Geach, T. J., Martin, A. C. R., Vacquier, V. D., Marchant, J. S., Dale, L. and Patel, S. (2008). Molecular characterization of a novel cell surface ADP-ribosyl cyclase from the sea urchin. *Cell. Signal.* **20**, 2347-2355.

Churchill, G. C., Okada, Y., Thomas, J. M., Genazzani, A. A., Patel, S. and Galione, A. (2002). NAADP mobilizes Ca(2+) from reserve granules, lysosome-related organelles, in sea urchin eggs. *Cell* **111**, 703-708.

Cuéllar-Mata, P., Martínez-Cadena, G., López-Godínez, J., Obregón, A. and García-Soto, J. (2000). The GTP-binding protein RhoA localizes to the cortical granules of *Strongylocentrotus purpuratus* sea urchin egg and is secreted during fertilization. *Eur. J. Cell Biol.* **79**, 81-91.

Davis, L. C. and Galione, A. (2013). Cytolytic granules supply Ca(2+) for their own exocytosis via NAADP and resident two-pore channels. *Commun. Integr. Biol.* **6**, e24175.

Davis, L. C., Morgan, A. J., Ruas, M., Wong, J. L., Graeff, R. M., Poustka, A. J., Lee, H. C., Wessel, G. M., Parrington, J. and Galione, A. (2008). Ca(2+) signaling occurs via second messenger release from intraorganelle synthesis sites. *Curr. Biol.* **18**, 1612-1618.

Davis, L. C., Morgan, A. J., Chen, J.-L., Snead, C. M., Bloor-Young, D., Shenderov, E., Stanton-Humphreys, M. N., Conway, S. J., Churchill, G. C., Parrington, J. et al. (2012). NAADP activates two-pore channels on T cell cytolytic granules to stimulate exocytosis and killing. *Curr. Biol.* **22**, 2331-2337.

Dunn, C. W., Howison, M. and Zapata, F. (2013). Agalma: an automated phylogenomics workflow. *BMC Bioinformatics* **14**, 330.

Guida, L., Bruzzone, S., Sturla, L., Franco, L., Zocchi, E. and De Flora, A. (2002). Equilibrative and concentrative nucleoside transporters mediate influx of extracellular cyclic ADP-ribose into 3T3 murine fibroblasts. *J. Biol. Chem.* **277**, 47097-47105.

Guse, A. H. (2012). Linking NAADP to ion channel activity: a unifying hypothesis. *Sci. Signal.* **5**, pe18.

Hara-Yokoyama, M., Kukimoto-Niino, M., Terasawa, K., Harumiya, S., Podyma-Inoue, K. A., Hino, N., Sakamoto, K., Itoh, S., Hashii, N., Hiruta, Y. et al. (2012). Tetrameric interaction of the ectoenzyme CD38 on the cell surface enables its catalytic and raft-association activities. *Structure* **20**, 1585-1595.

Henson, J. H., Beaulieu, S. M., Kaminer, B. and Begg, D. A. (1990). Differentiation of a calsequestrin-containing endoplasmic reticulum during sea urchin oogenesis. *Dev. Biol.* **142**, 255-269.

Holland, N. D. (1980). Electron microscopic study of the cortical reaction in eggs of the starfish (Patiria miniata). *Cell Tissue Res.* **205**, 67-76.

Hooper, **R., Churamani, D., Brailoiu, E., Taylor, C. W. and Patel, S.** (2011). Membrane topology of NAADP-sensitive two-pore channels and their regulation by N-linked glycosylation. *J. Biol. Chem.* **286**, 9141-9149.

Hylander, B. L. and Summers, R. G. (1982). An ultrastructural immunocytochemical localization of hyalin in the sea urchin egg. *Dev. Biol.* **93**, 368-380.

Kishimoto, T. (2011). A primer on meiotic resumption in starfish oocytes: the proposed signaling pathway triggered by maturation-inducing hormone. *Mol. Reprod. Dev.* **78**, 704-707.

Lee, H. C. (2001). Physiological functions of cyclic ADP-ribose and NAADP as calcium messengers. *Annu. Rev. Pharmacol. Toxicol.* **41**, 317-345.

Lee, H. C. (2012). Cyclic ADP-ribose and Nicotinic Acid Adenine Dinucleotide Phosphate (NAADP) as messengers for calcium mobilization. *J. Biol. Chem.* **287**, 31633-31640.

Lim, D., Kyozuka, K., Gragnaniello, G., Carafoli, E. and Santella, L. (2001). NAADP+ initiates the Ca2+ response during fertilization of starfish oocytes. *FASEB J.* **15**, 2257-2267.

Lu, Y., Hao, B., Graeff, R. and Yue, J. (2013a). NAADP/TPC2/Ca(2+) Signaling Inhibits Autophagy. *Commun. Integr. Biol.* **6**, e27595.

Lu, Y., Hao, B.-X., Graeff, R., Wong, C. W. M., Wu, W.-T. and Yue, J. (2013b). Two pore channel 2 (TPC2) inhibits autophagosomal-lysosomal fusion by alkalinizing lysosomal pH. *J. Biol. Chem.* **288**, 24247-24263.

Macgregor, A., Yamasaki, M., Rakovic, S., Sanders, L., Parkesh, R., Churchill, G. C., Galione, A. and Terrar, D. A. (2007). NAADP controls cross-talk between distinct Ca2+ stores in the heart. *J. Biol. Chem.* **282**, 15302-15311.

Moccia, F., Billington, R. A. and Santella, L. (2006a). Pharmacological characterization of NAADP-induced Ca2+ signals in starfish oocytes. *Biochem. Biophys. Res. Commun.* **348**, 329-336.

Moccia, F., Nusco, G. A., Lim, D., Kyozuka, K. and Santella, L. (2006b). NAADP and InsP3 play distinct roles at fertilization in starfish oocytes. *Dev. Biol.* **294**, 24-38.

Morgan, A. J. (2011). Sea urchin eggs in the acid reign. *Cell Calcium* **50**, 147-156.

Morgan, A. J. and Galione, A. (2007a). NAADP induces pH changes in the lumen of acidic Ca^{2+} stores. *Biochem. J.* **402**, 301-310.

Morgan, A. J. and Galione, A. (2007b). Fertilization and nicotinic acid adenine dinucleotide phosphate induce pH changes in acidic Ca(2+) stores in sea urchin eggs. *J. Biol. Chem.* **282**, 37730-37737.

Morgan, A. J. and Galione, A. (2014). Two-pore channels (TPCs): current controversies. *BioEssays* **36**, 173-183.

Morgan, A. J., Platt, F. M., Lloyd-Evans, E. and Galione, A. (2011). Molecular mechanisms of endolysosomal Ca^{2+} signalling in health and disease. *Biochem. J.* **439**, 349-374.

Morgan, A. J., Davis, L. C., Wagner, S. K. T. Y., Lewis, A. M., Parrington, J., Churchill, G. C. and Galione, A. (2013). Bidirectional Ca(2+) signaling occurs between the endoplasmic reticulum and acidic organelles. *J. Cell Biol.* **200**, 789-805.

Oulhen, N., Reich, A., Wong, J. L., Ramos, I. and Wessel, G. M. (2013). Diversity in the fertilization envelopes of echinoderms. *Evol. Dev.* **15**, 28-40.

Oulhen, N., Onorato, T. M., Ramos, I. and Wessel, G. M. (2014). Dysferlin is essential for endocytosis in the sea star oocyte. *Dev. Biol.* **388**, 94-102.

Parrington, J. and Tunn, R. (2014). Ca2+ signals, NAADP and two pore channels: role in cellular differentiation. *Acta Physiol.* **211**, 285-296.

Patel, S. and Docampo, R. (2010). Acidic calcium stores open for business: expanding the potential for intracellular Ca2+ signaling. *Trends Cell Biol.* **20**, 277-286.

Patel, S. and Muallem, S. (2011). Acidic Ca(2+) stores come to the fore. *Cell Calcium* **50**, 109-112.

Patel, S., Ramakrishnan, L., Rahman, T., Hamdoun, A., Marchant, J. S., Taylor, C. W. and Brailoiu, E. (2011). The endo-lysosomal system as an NAADP-sensitive acidic Ca(2+) store: role for the two-pore channels. *Cell Calcium* **50**, 157-167.

Peiter, E., Maathuis, F. J. M., Mills, L. N., Knight, H., Pelloux, J., Hetherington, A. M. and Sanders, D. (2005). The vacuolar Ca2+-activated channel TPC1 regulates germination and stomatal movement. *Nature* **434**, 404-408.

Pitt, S. J., Funnell, T. M., Sitsapesan, M., Venturi, E., Rietdorf, K., Ruas, M., Ganesan, A., Gosain, R., Churchill, G. C., Zhu, M. X. et al. (2010). TPC2 is a novel NAADP-sensitive Ca2+ release channel, operating as a dual sensor of luminal pH and Ca2+. *J. Biol. Chem.* **285**, 35039-35046.

Ploegh, H. L. (2007). A lipid-based model for the creation of an escape hatch from the endoplasmic reticulum. *Nature* **448**, 435-438.

Ramakrishnan, L., Muller-Steffner, H., Bosc, C., Vacquier, V. D., Schuber, F., Moutin, M.-J., Dale, L. and Patel, S. (2010). A single residue in a novel ADP-ribosyl cyclase controls production of the calcium-mobilizing messengers cyclic ADP-ribose and nicotinic acid adenine dinucleotide phosphate. *J. Biol. Chem.* **285**, 19900-19909.

Ramos, I. B., Miranda, K., Pace, D. A., Verbist, K. C., Lin, F.-Y., Zhang, Y., Oldfield, E., Machado, E. A., de Souza, W. and Docampo, R. (2010). Calcium- and polyphosphate-containing acidic granules of sea urchin eggs are similar to acidocalcisomes, but are not the targets for NAADP. *Biochem. J.* **429**, 485–495.

Reimer, C. L. and Crawford, B. J. (1995). Identification and partial characterization of yolk and cortical granule proteins in eggs and embryos of the starfish, Pisaster ochraceus. *Dev. Biol.* **167**, 439-457.

Ruas, M., Rietdorf, K., Arredouani, A., Davis, L. C., Lloyd-Evans, E., Koegel, H., Funnell, T. M., Morgan, A. J., Ward, J. A., Watanabe, K. et al. (2010). Purified TPC isoforms form NAADP receptors with distinct roles for Ca(2+) signaling and endolysosomal trafficking. *Curr. Biol.* **20**, 703-709.

Development (2014) 141, 4598-4609 doi:10.1242/dev.113563

Rybalchenko, V., Ahuja, M., Coblentz, J., Churamani, D., Patel, S., Kiselyov, K. and Muallem, S. (2012). Membrane potential regulates nicotinic acid adenine dinucleotide phosphate (NAADP) dependence of the pH- and Ca2+-sensitive organellar two-pore channel TPC1. *J. Biol. Chem.* **287**, 20407-20416.

Sánchez-Tusie, A. A., Vasudevan, S. R., Churchill, G. C., Nishigaki, T. and Treviño, C. L. (2014). Characterization of NAADP-mediated calcium signaling in human spermatozoa. *Biochem. Biophys. Res. Commun.* **443**, 531-536.

Santella, L., Kyozuka, K., Genazzani, A. A., De Riso, L. and Carafoli, E. (2000). Nicotinic acid adenine dinucleotide phosphate-induced Ca(2+) release. Interactions among distinct Ca(2+) mobilizing mechanisms in starfish oocytes. *J. Biol. Chem.* **275**, 8301-8306.

Schieder, M., Rotzer, K., Bruggemann, A., Biel, M. and Wahl-Schott, C. A. (2010). Characterization of two-pore channel 2 (TPCN2)-mediated Ca2+ currents in isolated lysosomes. *J. Biol. Chem.* **285**, 21219-21222.

Terasaki, M. and Jaffe, L. A. (1991). Organization of the sea urchin egg endoplasmic reticulum and its reorganization at fertilization. *J. Cell Biol.* **114**, 929-940.

Wang, X., Zhang, X., Dong, X.-P., Samie, M., Li, X., Cheng, X., Goschka, A., Shen, D., Zhou, Y., Harlow, J. et al. (2012). TPC Proteins Are Phosphoinositide-Activated Sodium-Selective Ion Channels in Endosomes and Lysosomes. *Cell* **151**, 372-383.

Wessel, G. M. (1989). Cortical granule-specific components are present within oocytes and accessory cells during sea urchin oogenesis. *J. Histochem. Cytochem.* **37**, 1409-1420.

Wessel, G. M., Brooks, J. M., Green, E., Haley, S., Voronina, E., Wong, J., Zaydfudim, V. and Conner, S. (2001). The biology of cortical granules. *Int. Rev. Cytol.* **209**, 117-206.

Wessel, G. M., Reich, A. and Klatsky, P. C. (2010). Use of sea stars to study basic reproductive processes. *Syst. Reprod. Biol.* **56**, 236-245.

Whitaker, M. (2006). Calcium at fertilization and in early development. *Physiol. Rev.* **86**, 25-88.

Zong, X., Schieder, M., Cuny, H., Fenske, S., Gruner, C., Rötzer, K., Griesbeck, O., Harz, H., Biel, M. and Wahl-Schott, C. (2009). The two-pore channel TPCN2 mediates NAADP-dependent Ca(2+)-release from lysosomal stores. *Pflugers Arch.* **458**, 891-899.

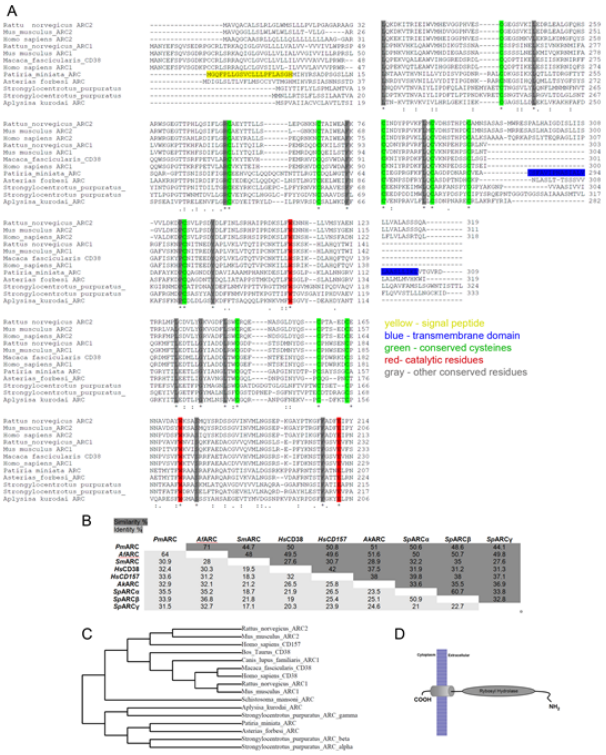

Figure S1: *P. miniata* ADP ribosyl cyclase (PmARC). One isoform of ARC was found in ovarian transcriptomes of *P. miniata*. **A,** Sequence alignment of ARC family proteins by ClustalW. Catalytic residues (red), conserved cysteines (green), identical residues (dark grey). The signal peptide (yellow) was predicted by SignalP 4.0 and the C-terminal transmembrane domain (blue) was predicted by TMHMM2. Putative sites for N-glysosylation (squares) were predicted by NetNGlyc 1.0. **B,** Percentage of identical (light grey) and similar (dark grey) residues amongst ARC proteins across species. Values relate to the alignment in (A). **C,** Phylogenetic relationship of cloned ARC proteins across different species using the Neighbor-Joining method by Phylotree. **D,** Predicted topology of mature *P. miniata* ARC protein. The ribosyl-hydrolase domain (Ribhydrolase) was predicted by Pfam (accession number PF02267) and transmembrane segment (cylinder) predicted by TMHMM2. *Hs: Homo sapiens, Sp: S. purpuratus, At: A. thaliana, Pm: P. miniata*, Af: *A. forbesi*, Ak: *A. kurodai*, Rn: *R. norvegicus*, Sm: *S. mansoni*, Mm, *M. musculus*, Mf: *M. fascicularis.*

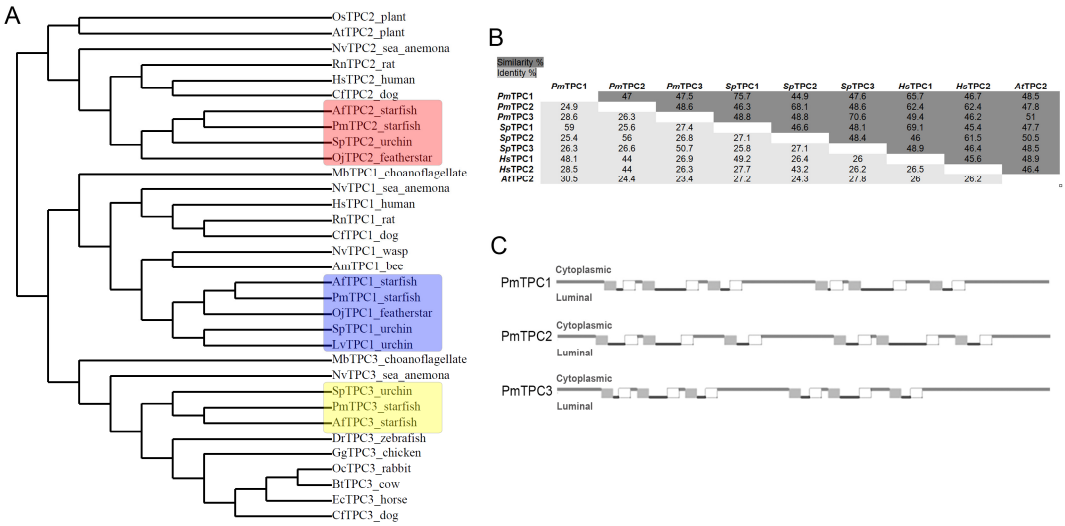

Figure S2: *P. miniata* Two-Pore Channels (PmTPCs). Three isoforms of TPCs were found in ovarian transcriptomes of *P. miniata* (PmTPC1, PmTPC2 and PmTPC3). **A,** Phylogenetic relationship of cloned PmTPCs across different species using the Neighbor-Joining method by Phylotree. **B,** Percentage of identical (light grey) and similar (dark grey) residues amongst TPC proteins across species. Values relate to the alignment in (A). **C,** Predicted topology of mature *P. miniata* TPCs. Transmembrane segments (cylinders) were predicted by TopCons server. *Hs: Homo sapiens, Sp: S. purpuratus, At: A. thaliana, Pm: P. miniata*, Af: *A. forbesi*, Oj: *O. japonicus*, Lv: *L. variegatus*, Mb: *M. brevicollis,* Nv: *N. vectensis,* Rn: *Rattus norvegicus,* Cf: *C. familiaris,* Am: *A. mellifera,* Dr: *D. rerio,* Gg: *G. gallus,* Oc: *O. cuniculus,* Bt: *B. Taurus,* Ec: *E. caballus.*

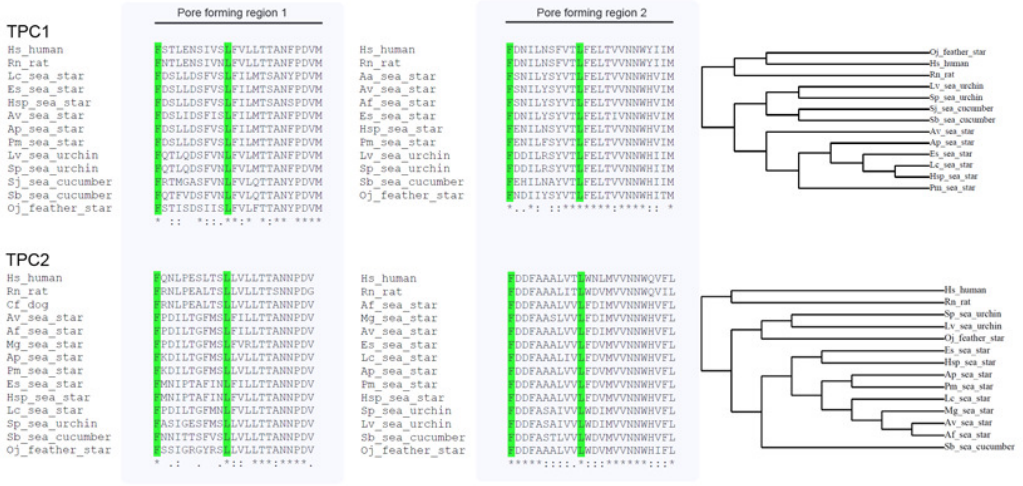

Figure S3: Alignment of TPCs 1 and 2 putative pore forming regions from human, rat and different echinoderms. Residues in green are conserved between the pores and across the species. Lc, *L. clathrata*; Es, *E. spinulosus*; Av, *A. vulgaris (A. rubens)*; Ap, *A. pectinifera (P. pectinifera)*; Pm, *P. miniata*; Lv, *L. variegatus*; Sp, *S. purpuratus*; Sj, *S. japonicus (A. japonicus)*; Sb, *S. briareus*; Oj, *O. japonicus*; Hsp, *Henricia* species; Af, *A. forbesi*; Rn, *R. norvegicus*; Cf, *C. familiaris*, Hs, *H. sapiens.*

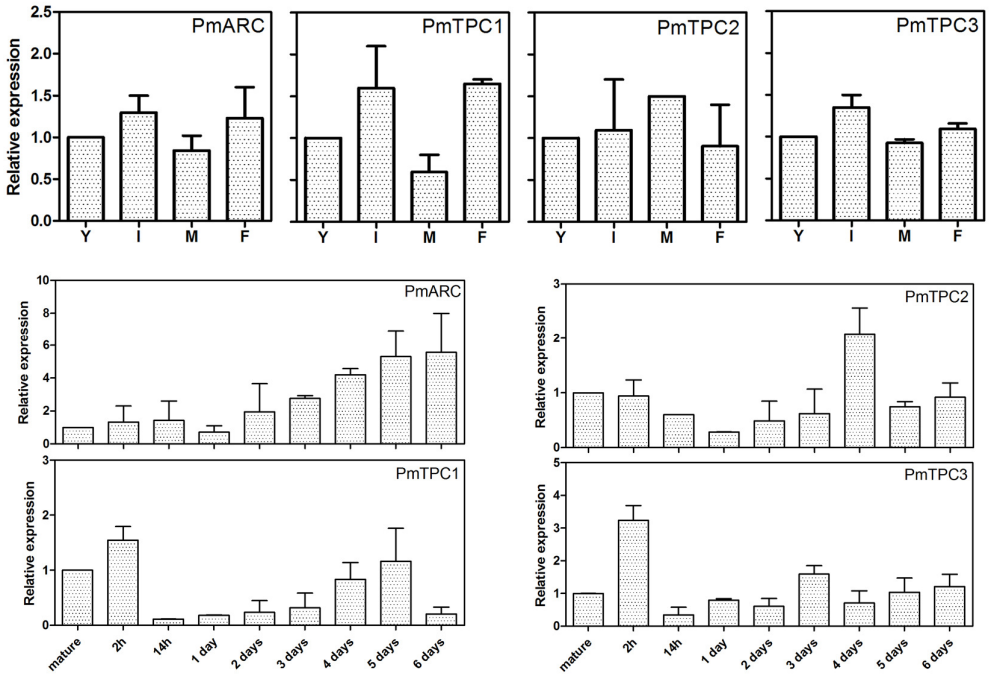

Figure S4: qPCR for PmARC and PmTPCs isoforms throughout oogenesis and early embryogenesis of *P. miniata*. RNA was extracted from different stages of oogenesis and embryogenesis and gene expression was accessed by Real-Time PCR. Values are normalized by the levels of *P. miniata* Ubiquitin cDNA. Oogenesis: (Y) young oocyte 50-100 μm in diameter, (I) full grown immature oocyte, (M) mature egg, (F) egg 30 min after fertilization. Embryogenesis: mature egg, followed by embryos hours and days after fertilization as indicated in the image. Graphs show the mean (± 1 S.D.) of at least three experiments.

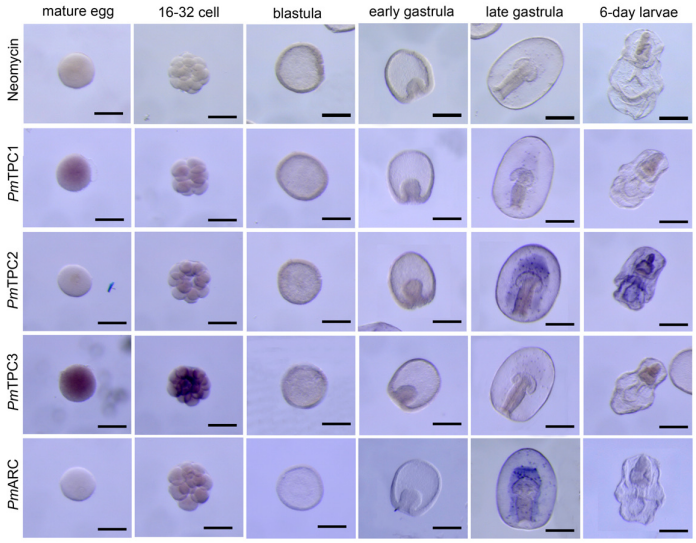

Figure S5: Whole mount *In situ* hybridizations for PmARC and PmTPC isoforms in *P. miniata* eggs and embryos. Neomycin was used as a negative control for staining. Embryonic stages are indicated in the image. Bars: 180 μm.

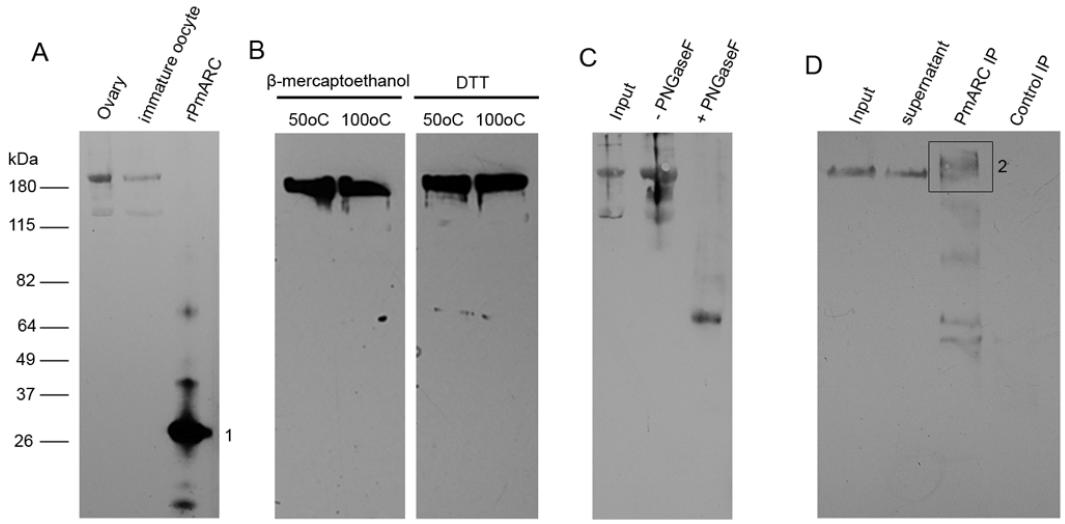

Figure S6: PmARC immunoblotings in different conditions. A, endogenous PmARC from oocytes, ovaries and rPmARC. Note the difference in molecular weight. **B,** immature oocytes samples were prepared using lower heating and different reducing agents before loading in the gel. **C,** PNGase treatment of immature oocytes samples. **D,** immunoprecipitation of PmARC followed by immunoblotting. Samples marked 1 (in **A**) and 2 (in **D**) were excised from the gel and analyzed my mass spectrometry.

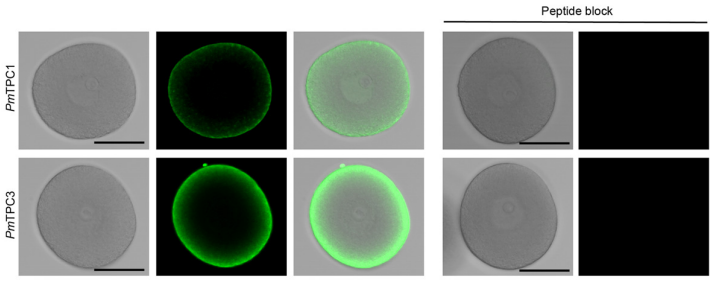

Figure S7: Peptide-block immunolocalization of PmTPCs 1 and 2. Oocytes were pre-incubated with 1 mg/ml of each of the peptides from the cocktail used to raise the antibodies in rabbits and processed for immunolocalization Bars: 150 μm.

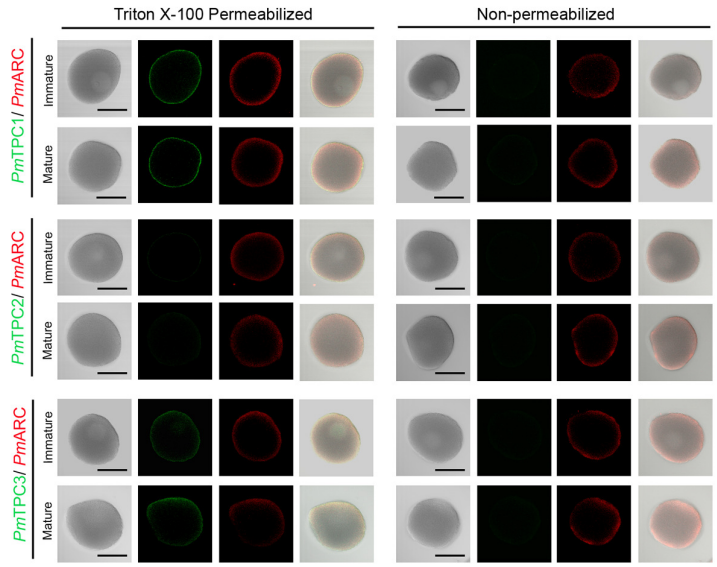

Figure S8: Colocalization of PmTPCs and PmARC in immature oocytes and mature eggs with or without Triton X-100 permeabilization. Note that PmTPCs signals decrease but are still detectable whereas PmARC signals are only slightly affected in non-permeabilized oocytes and eggs. Bars: 150 µm.

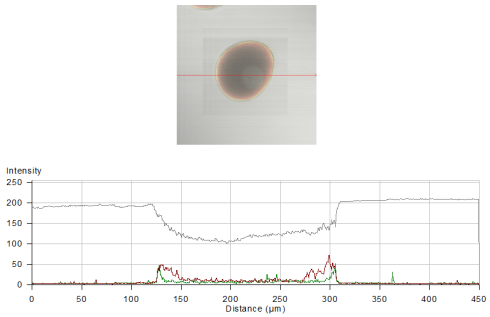

Figure S9: Intensity line Plot for PmTPC3 and PmARC immunolocalization signals. PmTPC3, green signal; PmARC, red signal, Bright field, gray signal.

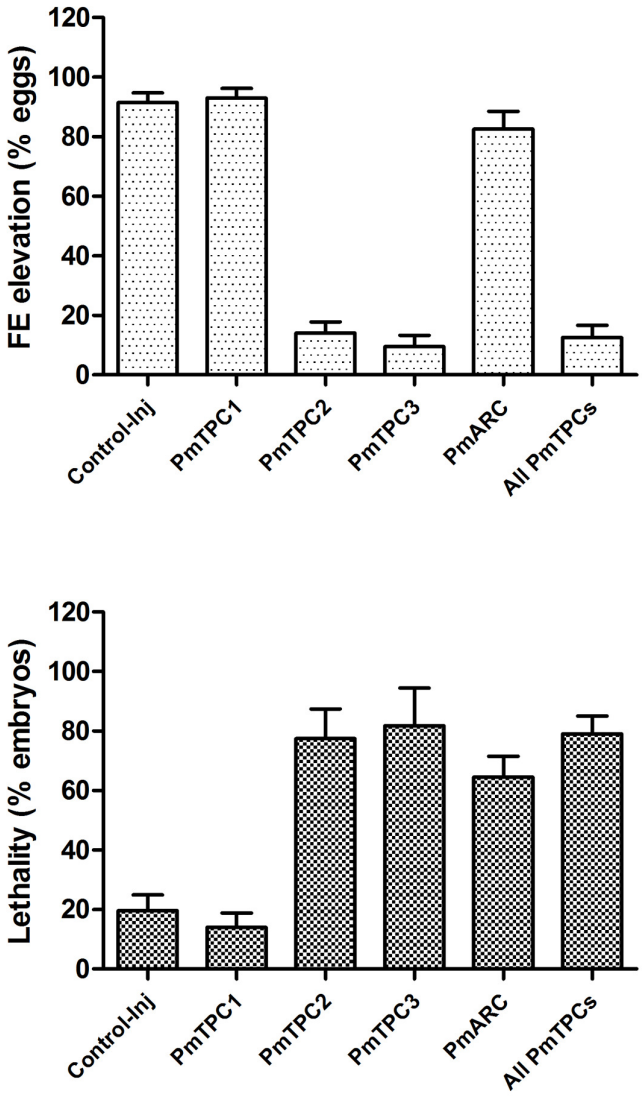

Figure S10: Morpholino phenotypes quantifications. Percentages of embryos presenting the fertilization envelope phenotype and lethality after gastrulation in the different morpholino knockdown experiments (n=6).

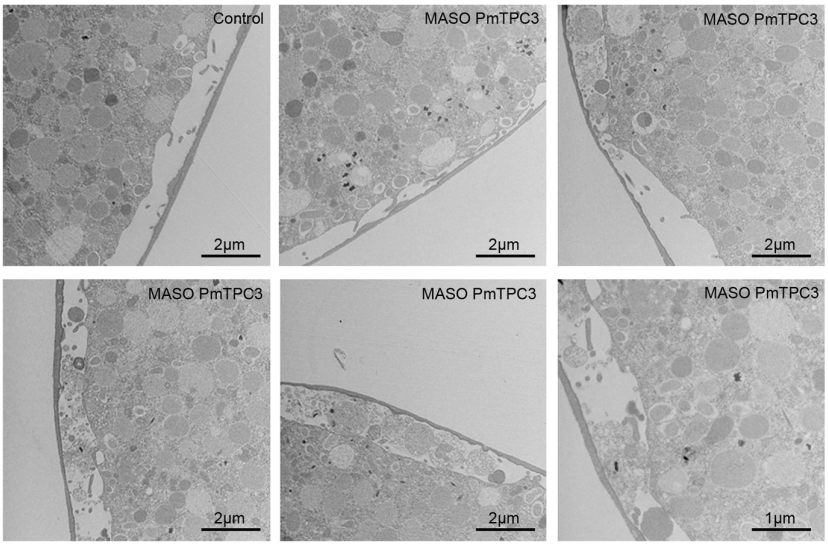

Figure S11: PmTPC3-knockdown eggs 10 min after fertilization. Collection of TEM images of the cortices and fertilization envelopes of PmTPC3 knockdown eggs.

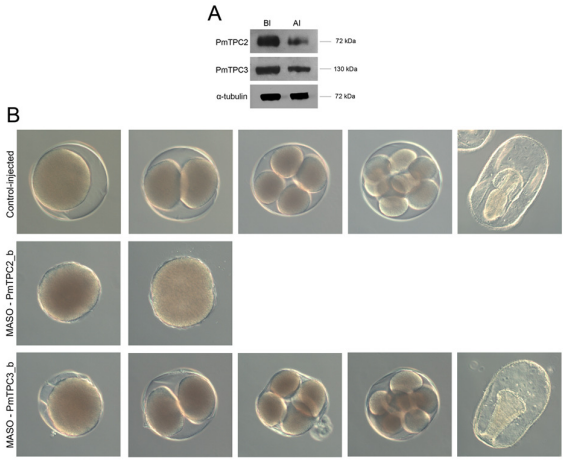

Figure S12: Eggs and embryos after injections of morpholinos directed to different regions of the 5'UTR of PmTPCs 2 and 3. A, Immunoblotting before and after morpholino injections. **B,** Control and injected eggs and embryos at first cleavage, 8-16, 16-32 cell stage, and gastrulation.

Movie 1: Global calcium signals at fertilization in sea stars. Control eggs and eggs co-injected with all three PmTPCs morpholinos. Control calcium signals and the two phenotypes described in Figure 5 are shown.

Table S1: Primers, peptides and morpholinos.

Primers and Peptides	**Sequence**
5´and 3´ RACEs	
PmARC 5'RACE outer	5'- CGGAGCCAAGCAGGGGGAACTGTC-3'
PmARC 5'RACE inner	5'- GACTGGATGAAAGATGCCGGGGGTTG-3´
PmTPC1 5'RACE outer	5'- CGTGATACGAAAATGGCTCCGTTGCCTG-3'
PmTPC1 5'RACE inner	5'- CAAGGACGACGATGGCTTCACAGAAC-3
PmTPC1 3'RACE outer	5'- GGAAACCGGCCACCACAATGACAGCG-3'
PmTPC1 3'RACE inner	5'- GACAATGACAGCACGACCGCGTGCCAGC-3'
PmTPC2 5'RACE outer	5'- CGACTCCGAGGATCTACGACCAGGATGG-3'
PmTPC2 5'RACE inner	5'- GGGATTCATCGTAACTACTCGGTCTGCCT -3'
PmTPC2 3'RACE outer	5'- GACATCTACGCCTCTGATCTCAGGGG-3'
PmTPC2 3'RACE inner	5'- CTCTACGCCGAGACCGAACAGCCAATGC-3'
PmTPC3 5'RACE outer	5'- GCGGAAGACTTTCTCATCACTCCCGTTTCC-3'
PmTPC3 5'RACE inner	5'- CAAGGATGGTGACAACAAGCATATCCAC-3'
PmTPC3 3'RACE outer	5'- GGAATCCGCTTCCGCATTGGAAAGAAATCC-3'
PmTPC3 3'RACE inner	5'- GAAATGTACAGGTGTCGTTGCAGGCCATG-3'
qPCR	
ForPmARC	5'-GCTGTGTGATAAAGGCAGCA-3'
RevPmARC	5'-GCCAGGACCAATGCAATACT-3'
ForPmTPC1	5'-ATCCTGGAGGCCTTTGTCTT-3'
RevPmTPC1	5'-TGCTTTGGTCCTTTTTCTGG-3'
ForPmTPC2	5'-TTGCTAGCGTGCTTTTGCTA-3'
RevPmTPC2	5'-GGCCATTGGCATATGTAACC-3'
ForPmTPC3	5'-CGACAGCAAGTTTGTCCTGA-3'
RevPmTPC3	5'-CGGTGGACAGTCTGACATTG-3'
ForPmUbiquitin	5'-TTCGGTGAAAGCCAAGATTC-3'
RevPmUbiquitin	5'-CCCACCTCTCATGGCTAGAA-3
***In situ* probes**	
ForIsPmARC	5'-GAGGGCCGACCACGTCTAACATAAGC-3'
RevIsPmARC	5'-CTAGAAATGTAGTGAGTTCGGCGATTC-3'
ForIsPmTPC1	5'-TTAGCGGTAGTATACGACACTTTCAC-3'
RevIsPmTPC1	5'-AAAGAACGACTCGTAGGTTGTATTCT-3'
ForIsPmTPC2	5'-GCTGTCAAGTATCGAAGTATAAACCA-3'
RevIsPmTPC2	5'-TGAAGAAAAAGTACAGTCCAATGAC-3'
ForIsPmTPC3	5'-GTACGCCATTCTTTCAGAAGTACATA-3'
RevIsPmTPC3	5'-CCAACTCATCAATCTTCTTTTCAATA-3'
Morpholinos	
PmARC:	5'-GGAACTGTCCCATGACTGGATGAAA-3'
PmTPC1	5'-TGGACTTGTTAAATCGTTCATGGTT-3'
PmTPC2	5'-TGATGTTTTTTCATCAAAGCCAGCA-3'
PmTPC3	5'-GTTTTCTTCACCATCAAGTCATCGC-3'
PmTPC2b	5'-AAAGCCAGCAAACGCAGTGTTCGGA-3'
PmTPC3b	5'-ATTACGTCGTTTCACTTTCAGACTC-3'
Antibodies Peptides	
PmTPC1	NH2-YLKEGENNHNFSTHPKSQDC-CONH2
	NH2-VQLKWKLKQDENRLWFEEC-CONH2
	NH2-ADEIKEWVREQDQTQRQDLQQC-CONH2
PmTPC2:	NH2-ELRGRPSSYDESLDRIHPGRRSSESC-CONH2

	NH2-DRDTSRRRKPPIVPKNNHILRKIC-CONH2
	NH2-WDREQQLEASEDPNNQPSYC-CONH2
PmTPC3	NH2-ADLMRERKGSVVRPRSVSFKKC-CONH2
	NH2-NRSTPFFQKYIPSCYNSRVSEFIC-CONH2
	NH2-EENMGPEELDDIDEMNPYENEPIC-CONH2
PmARC	NH2-CEEHVQCLQQDQCNTNT-CONH2
	NH2-GINYDTPCPSAYSSGC-CONH2
	NH2-TMYTFWRAASRAFARQATGC-CONH2

Table S2: Protein Groups and Peptide-Spectrum Matches (PSMs) for the rPmARC and the immunoprecipteted endogenous PmARC after immunoblotting detecetion.

Protein Groups and Peptide-Spectrum Matches (PSMs)				
Sample ID	***Accession Number***	***Protein Name***	***Protein Score***	***Unique PSMs***
1 - rPmARC	Pm56316_0_T_1	Locus_56316.0_Transcript_1/0_Con_3_Len_2051 ~RPKM~2.96~NADA_APLCA~2e-43~ADP-ribosyl_cyclase_maxframe_1080	293.44	K.DESLFWSGLPK.L K.LALNNGR.V R.CEEHVQCLQQDQCNTNTTLR.G K.DLQTLLTDR.G R.QATGTISVALDGSR.T
2 - PmARC IP 182kDa	Pm56316_0_T_1	Locus_56316.0_Transcript_1/0_Con_3_Len_2051 ~RPKM~2.96~NADA_APLCA~2e-43~ADP-ribosyl_cyclase_maxframe_1080	286.78	K.DESLFWSGLPK.L K.LALNNGR.V K.LALNNGRVTGR.Y R.CEEHVQCLQQDQCNTNTTLR.G R.QATGTISVALDGSR.T

Sample ID, numbers 1 and 2 refer to the bands from Figure S6. **Accession Nr.,** accession number from the searched database (DB). **Protein Name,** protein name in the DB. **Protein Score,** sum of the contributing peptide scores. **Unique PSMs,** unique peptide-spectrum matches that contribute to the protein assignment.